PTEP

Prog. Theor. Exp. Phys. **2022** 043B04(21 pages)
DOI: 10.1093/ptep/ptac052

Anomaly flow by an Aharonov–Bohm phase

Shuichiro Funatsu[1], Hisaki Hatanaka[2], Yutaka Hosotani[3], Yuta Orikasa[4], and Naoki Yamatsu[5]

[1]*Institute for Promotion of Higher Education, Kobe University, Kobe 657-0011, Japan*
[2]*Osaka, Osaka 536-0014, Japan*
[3]*Department of Physics, Osaka University, Toyonaka, Osaka 560-0043, Japan*
[4]*Institute of Experimental and Applied Physics, Czech Technical University in Prague, Husova 240/5, 110 00 Prague 1, Czech Republic*
[5]*Department of Physics, Kyushu University, Fukuoka 819-0395, Japan*
*E-mail: hosotani@het.phys.sci.osaka-u.ac.jp

Received February 4, 2022; Revised March 11, 2022; Accepted March 16, 2022; Published March 21, 2022

In gauge-Higgs unification (GHU), gauge symmetry is dynamically broken by an Aharonov–Bohm (AB) phase, θ_H, in the fifth dimension. We analyze $SU(2)$ GHU with an $SU(2)$ doublet fermion in the flat $M^4 \times (S^1/Z_2)$ spacetime and in the Randall–Sundrum (RS) warped space. With orbifold boundary conditions the $U(1)$ part of gauge symmetry remains unbroken at $\theta_H = 0$ and π. The fermion multiplet has chiral zero modes at $\theta_H = 0$, which become massive at $\theta_H = \pi$. In other words, chiral fermions are transformed to vector-like fermions by the AB phase θ_H. The chiral anomaly at $\theta_H = 0$ continuously varies as θ_H, and vanishes at $\theta_H = \pi$. We demonstrate this intriguing phenomenon in the RS space in which no level crossing occurs in the mass spectrum and everything varies smoothly. The flat spacetime limit is singular as the anti-de Sitter curvature of the RS space diminishes, and reproduces the result in the flat spacetime. Anomalies appear for various combinations of Kaluza–Klein excitation modes of gauge fields as well. Although the magnitude of the anomalies depends on θ_H and the warp factor of the RS space, it does not depend on the bulk mass parameter of the fermion field controlling its mass and wave function at general θ_H.

Subject Index B00, B06, B31, B40, B43

1. Introduction

In gauge-Higgs unification (GHU), gauge symmetry is dynamically broken by an Aharonov–Bohm (AB) phase, θ_H, in the fifth dimension [1–7]. In the analysis of the finite-temperature behavior of the grand unified theory inspired $SO(5) \times U(1)_X \times SU(3)_C$ GHU models in the Randall–Sundrum (RS) warped space, it has been observed that chiral quarks and leptons at $\theta_H = 0$ are transformed to vector-like fermions at $\theta_H = \pi$ [8]. As θ_H varies from 0 to π, $SU(2)_L \times U(1)_Y \times SU(3)_C$ gauge symmetry is smoothly converted to $SU(2)_R \times U(1)_{Y'} \times SU(3)_C$ gauge symmetry. Chiral fermions appearing as zero modes of fermion multiplets in the spinor representation of $SO(5)$ at $\theta_H = 0$ become massive fermions having vector-like gauge couplings at $\theta_H = \pi$.

In general, chiral fermions in four dimensions give rise to chiral anomalies [9–12]. What would be the fate of those anomalies if fermions are converted to massive vector-like fermions at $\theta_H = \pi$? Do anomalies disappear as θ_H changes from 0 to π? How can it happen? These are the questions and issues addressed in this paper.

Funded by SCOAP[3]

To keep the arguments clear, we analyze $SU(2)$ GHU with an $SU(2)$ doublet fermion both in the flat $M^4 \times (S^1/Z_2)$ spacetime and in the RS warped space with orbifold boundary conditions breaking $SU(2)$ to $U(1)$. We shall see that $U(1)$ gauge symmetry survives at $\theta_H = 0$ and π, and that the fermion multiplet has chiral zero modes at $\theta_H = 0$ which become massive at $\theta_H = \pi$. We determine four-dimensional (4D) couplings of all Kaluza–Klein (KK) modes of gauge fields and fermion fields at general θ_H, and evaluate triangle chiral anomalies.

In the flat $M^4 \times (S^1/Z_2)$ spacetime all gauge couplings are determined analytically, but the mass spectrum of gauge and fermion fields exhibits level crossing as θ_H varies. In the RS spacetime no level crossing occurs in the spectrum, and gauge couplings are evaluated numerically. It will be seen that 4D gauge couplings of fermions in the RS space smoothly change with θ_H, and that the chiral anomaly associated with the zero mode of gauge fields at $\theta_H = 0$ smoothly varies and vanishes at $\theta_H = \pi$. The flat-space limit gives singular behavior of the anomaly as a function of θ_H, reproducing the analytical result in the flat spacetime. We will also see that anomalies appear in various combinations of KK modes of gauge fields.

In Sect. 2 $SU(2)$ GHU models are introduced in both the flat $M^4 \times (S^1/Z_2)$ spacetime and in the RS space. As functions of the AB phase θ_H the mass spectra of the KK modes of gauge and fermion fields are obtained. It will be seen that no level crossing occurs in the spectrum in the RS space. In Sect. 3 gauge couplings and anomalies are evaluated in the flat $M^4 \times (S^1/Z_2)$ spacetime. In Sect. 4 gauge couplings and anomalies are evaluated in the RS space. It is shown that the magnitudes of anomalies smoothly change with θ_H. The dependence of those anomalies on the warp factor z_L of the RS space and the bulk mass parameter c of fermion fields is also investigated. It is seen that the flat space limit $z_L \to 1$ of anomalies is singular. It is also seen by numerical evaluation that the magnitude of anomalies does not depend on the bulk mass parameter c. Section 5 is devoted to a summary and discussion.

2. *SU*(2) GHU models

The action in $SU(2)$ GHU in the flat $M^4 \times (S^1/Z_2)$ spacetime with coordinate x^M ($M = 0, 1, 2, 3, 5$, $x^5 = y$) is given by

$$
\begin{aligned}
I_{\text{flat}} &= \int d^4x \int_0^L dy \mathcal{L}_{\text{flat}}, \\
\mathcal{L}_{\text{flat}} &= -\frac{1}{2}\text{Tr}\, F_{MN}F^{MN} + \overline{\Psi}\gamma^M D_M \Psi + \overline{\Psi}'\gamma^M D_M \Psi',
\end{aligned} \tag{1}
$$

where $\mathcal{L}_{\text{flat}}(x^\mu, y) = \mathcal{L}_{\text{flat}}(x^\mu, -y) = \mathcal{L}_{\text{flat}}(x^\mu, y + 2L)$. Here,

$$
F_{MN} = \partial_M A_N - \partial_N A_N - ig_A[A_M, A_N],
$$

with $A_M = \frac{1}{2}\sum_{a=1}^3 A_M^a \tau^a$, where the τ^a are Pauli matrices. We have introduced two types of $SU(2)$ doublet fermions Ψ, Ψ' with $D_M = \partial_M - ig_A A_M$. The metric is $\eta_{MN} = \text{diag}\,(-1, 1, 1, 1, 1)$ and $\overline{\Psi} = i\Psi^\dagger\gamma^0$. Orbifold boundary conditions are given, with $(y_0, y_1) = (0, L)$, by

$$
\begin{aligned}
\begin{pmatrix} A_\mu \\ A_y \end{pmatrix}(x, y_j - y) &= P_j \begin{pmatrix} A_\mu \\ -A_y \end{pmatrix}(x, y_j + y)P_j^{-1}, \\
\Psi(x, y_j - y) &= P_j\gamma^5\Psi(x, y_j + y), \\
\Psi'(x, y_j - y) &= (-1)^j P_j\gamma^5\Psi'(x, y_j + y), \\
P_0 = P_1 &= \tau^3.
\end{aligned} \tag{2}
$$

The $SU(2)$ symmetry is broken to $U(1)$ by the boundary conditions in Eq. (2). A_μ^3 and $A_y^{1,2}$ are parity even at both y_0 and y_1, and have constant zero modes. Let us denote doublet fields as $\Psi = (u, d)^t$ and $\Psi' = (u', d')^t$. u_R and d_L are parity even at both y_0 and y_1, and have zero modes, leading to chiral structure.

The KK expansions of gauge fields around the configuration $A_M = 0$ are given, with $L = \pi R$, by

$$\begin{aligned}
A_\mu^{1,2}(x,y) &= \sqrt{\frac{2}{\pi R}} \sum_{n=1}^{\infty} A_\mu^{1,2\,(n)}(x)\, \sin\frac{ny}{R}, \\
A_\mu^{3}(x,y) &= \frac{1}{\sqrt{\pi R}} A_\mu^{3\,(0)}(x) + \sqrt{\frac{2}{\pi R}} \sum_{n=1}^{\infty} A_\mu^{3\,(n)}(x)\, \cos\frac{ny}{R}, \\
A_y^{1,2}(x,y) &= \frac{1}{\sqrt{\pi R}} A_y^{1,2\,(0)}(x) + \sqrt{\frac{2}{\pi R}} \sum_{n=1}^{\infty} A_y^{1,2\,(n)}(x)\, \cos\frac{ny}{R}, \\
A_y^{3}(x,y) &= \sqrt{\frac{2}{\pi R}} \sum_{n=1}^{\infty} A_y^{3\,(n)}(x)\, \sin\frac{ny}{R}.
\end{aligned} \tag{3}$$

The gauge coupling of the 4D $U(1)$ gauge fields $A_\mu^{3\,(0)}(x)$ is given by

$$g_4 = \frac{g_A}{\sqrt{L}}. \tag{4}$$

The zero modes $A_y^{1,2\,(0)}$ may develop a nonvanishing expectation value, which leads to an AB phase θ_H along the fifth dimension. Without loss of generality one may assume that $\langle A_y^{1\,(0)} \rangle = 0$. Then

$$P \exp\left\{ ig_A \int_0^{2L} dy\, \langle A_y \rangle \right\} = e^{i\theta_H \tau^2} = \begin{pmatrix} \cos\theta_H & \sin\theta_H \\ -\sin\theta_H & \cos\theta_H \end{pmatrix}, \qquad \theta_H = g_4 L\, \langle A_y^{2\,(0)} \rangle. \tag{5}$$

The AB phase θ_H is a physical quantity. It couples to fields, affecting their mass spectrum. It will be shown shortly that the mode expansions in Eq. (3) do not correspond to mass eigenstates for $\theta_H \neq 0$ and need to be improved.

One can change the value of θ_H by a gauge transformation, which also alters boundary conditions. Consider a large gauge transformation given by

$$\begin{aligned}
&\tilde{A}_M = \Omega A_M \Omega^{-1} + \frac{i}{g_A} \Omega \partial_M \Omega^{-1}, \qquad \tilde{\Psi} = \Omega \Psi, \qquad \tilde{\Psi}' = \Omega \Psi', \\
&\Omega = \exp\left(\frac{i}{2} \theta(y) \tau^2 \right), \qquad \theta(y) = \theta_H \left(1 - \frac{y}{L} \right),
\end{aligned} \tag{6}$$

under which $\tilde{\theta}_H = 0$ and the boundary condition matrices become

$$\tilde{P}_j = \Omega(y_j - y) P_j \Omega^{-1}(y_j + y), \qquad \tilde{P}_0 = \begin{pmatrix} \cos\theta_H & -\sin\theta_H \\ -\sin\theta_H & -\cos\theta_H \end{pmatrix}, \qquad \tilde{P}_1 = \tau^3. \tag{7}$$

Although the AB phase $\tilde{\theta}_H$ vanishes, the boundary conditions become nontrivial; the physics remains the same. This gauge is called the twisted gauge [13,14].

In the twisted gauge $\tilde{\theta}_H = 0$, so that fields satisfy free equations. The boundary condition at $y = L$ remains the same as in the original gauge so that mode functions take the form

$$\begin{aligned}
\tilde{P}_1 = +: &\quad C_\lambda(y) = \cos\lambda(y - L), \\
\tilde{P}_1 = -: &\quad S_\lambda(y) = \sin\lambda(y - L).
\end{aligned} \tag{8}$$

At $y = 0$, $\tilde{A}^1_\mu$ and $\tilde{A}^3_\mu$ intertwine with each other. Their general eigenmodes can be written in the form

$$\begin{pmatrix} \tilde{A}^1_\mu \\ \tilde{A}^3_\mu \end{pmatrix} = \begin{pmatrix} \alpha S_\lambda(y) \\ \beta C_\lambda(y) \end{pmatrix} B^{(\lambda)}_\mu(x). \tag{9}$$

Note that

$$\begin{pmatrix} A^1_\mu \\ A^3_\mu \end{pmatrix} = \begin{pmatrix} \cos\theta(y) & \sin\theta(y) \\ -\sin\theta(y) & \cos\theta(y) \end{pmatrix} \begin{pmatrix} \tilde{A}^1_\mu \\ \tilde{A}^3_\mu \end{pmatrix}. \tag{10}$$

Hence, the boundary conditions at $y = 0$, which may be expressed as $A^1_\mu(x, 0) = 0$ and $(\partial A^3_\mu/\partial y)(x, 0) = 0$, lead to the condition

$$\begin{pmatrix} c_H S_\lambda(0) & s_H C_\lambda(0) \\ -s_H S'_\lambda(0) & c_H C'_\lambda(0) \end{pmatrix} \begin{pmatrix} \alpha \\ \beta \end{pmatrix} = 0, \tag{11}$$

where $c_H = \cos\theta_H$ and $s_H = \sin\theta_H$. The eigenvalues λ must satisfy $c^2_H S_\lambda C'_\lambda + s^2_H C_\lambda S'_\lambda\big|_{y=0} = 0$, or

$$\sin^2 \lambda\pi R - \sin^2\theta_H = 0, \tag{12}$$

which leads to the spectrum for λ: $\{R^{-1}(n \pm \theta_H/\pi) \geq 0;\ n : \text{integers})\}$. Zero ($\lambda = 0$) modes appear for $\sin\theta_H = 0$. The coefficients α and β for each mode are determined by Eq. (11) as well. KK expansions for $\tilde{A}^1_\mu$, and $\tilde{A}^3_\mu$ are expressed in the form

$$\begin{pmatrix} \tilde{A}^1_\mu(x, y) \\ \tilde{A}^3_\mu(x, y) \end{pmatrix} = \sum_{n=-\infty}^{\infty} B^{\langle n\rangle}_\mu(x) \frac{1}{\sqrt{\pi R}} \begin{pmatrix} \sin\left[\dfrac{ny}{R} - \theta(y)\right] \\ \cos\left[\dfrac{ny}{R} - \theta(y)\right] \end{pmatrix}. \tag{13}$$

The mass of the $B^{\langle n\rangle}_\mu(x)$ mode is $m_n(\theta_H) = R^{-1}\left|n + \frac{\theta_H}{\pi}\right|$. In flat space the KK expansion takes a simpler form in the original gauge:

$$\begin{pmatrix} A^1_\mu(x, y) \\ A^3_\mu(x, y) \end{pmatrix} = \sum_{n=-\infty}^{\infty} B^{\langle n\rangle}_\mu(x) \frac{1}{\sqrt{\pi R}} \begin{pmatrix} \sin\dfrac{ny}{R} \\ \cos\dfrac{ny}{R} \end{pmatrix}. \tag{14}$$

The field $A^2_\mu(x, y)$ is not affected by θ_H, whose KK expansion is given by that in Eq. (3).

The fermion field Ψ in the twisted gauge,

$$\tilde{\Psi} = \begin{pmatrix} \tilde{u} \\ \tilde{d} \end{pmatrix} = \begin{pmatrix} \cos\frac{1}{2}\theta(y) & \sin\frac{1}{2}\theta(y) \\ -\sin\frac{1}{2}\theta(y) & \cos\frac{1}{2}\theta(y) \end{pmatrix} \begin{pmatrix} u \\ d \end{pmatrix}, \tag{15}$$

satisfies free equations in the bulk region $0 < y < L$ and the original boundary condition at $y = L$, so that its eigenmode takes the form

$$\begin{aligned} \begin{pmatrix} \tilde{u}_R \\ \tilde{d}_R \end{pmatrix}(x, y) &= \begin{pmatrix} \alpha_R C_\lambda(y) \\ \beta_R S_\lambda(y) \end{pmatrix} f_{\lambda,R}(x), \\ \begin{pmatrix} \tilde{u}_L \\ \tilde{d}_L \end{pmatrix}(x, y) &= \begin{pmatrix} \alpha_L S_\lambda(y) \\ -\beta_L C_\lambda(y) \end{pmatrix} f_{\lambda,L}(x), \\ \bar{\sigma}^\mu \partial_\mu f_{\lambda,R}(x) = \lambda f_{\lambda,L}(x), &\qquad \sigma^\mu \partial_\mu f_{\lambda,L}(x) = \lambda f_{\lambda,R}(x), \end{aligned} \tag{16}$$

where $\sigma^\mu = (I_2, \vec{\sigma})$ and $\bar{\sigma}^\mu = (-I_2, \vec{\sigma})$. It follows from the equations of motion in the bulk that $(\alpha_R, \beta_R) = (\alpha_L, \beta_L)$. The boundary conditions $(\partial u_R/\partial y)(x, 0) = 0$ and $d_R(x, 0) = 0$ lead to

$$\begin{pmatrix} \bar{s}_H C_\lambda(0) & \bar{c}_H S_\lambda(0) \\ \bar{c}_H C'_\lambda(0) & -\bar{s}_H S'_\lambda(0) \end{pmatrix} \begin{pmatrix} \alpha_R \\ \beta_R \end{pmatrix} = 0, \tag{17}$$

where $\bar{c}_H = \cos\frac{1}{2}\theta_H$ and $\bar{s}_H = \sin\frac{1}{2}\theta_H$. The eigenvalues λ must satisfy

$$\sin^2 \lambda\pi R - \sin^2 \tfrac{1}{2}\theta_H = 0, \tag{18}$$

which leads to the spectrum for λ: $\{R^{-1}(n \pm \theta_H/2\pi) \geq 0;\ n : \text{integers})\}$. Zero ($\lambda = 0$) modes appear for $\sin\frac{1}{2}\theta_H = 0$. The coefficients α_R and β_R for each mode are determined by Eq. (17). The KK expansion for $\tilde{\Psi}$ is given by

$$\begin{aligned} \begin{pmatrix} \tilde{u}_R(x, y) \\ \tilde{d}_R(x, y) \end{pmatrix} &= \sum_{n=-\infty}^{\infty} \psi_R^{\langle n \rangle}(x) \frac{1}{\sqrt{\pi R}} \begin{pmatrix} \cos\left[\dfrac{ny}{R} - \frac{1}{2}\theta(y)\right] \\ \sin\left[\dfrac{ny}{R} - \frac{1}{2}\theta(y)\right] \end{pmatrix}, \\ \begin{pmatrix} \tilde{u}_L(x, y) \\ \tilde{d}_L(x, y) \end{pmatrix} &= \sum_{n=-\infty}^{\infty} \psi_L^{\langle n \rangle}(x) \frac{1}{\sqrt{\pi R}} \begin{pmatrix} \sin\left[\dfrac{ny}{R} - \frac{1}{2}\theta(y)\right] \\ -\cos\left[\dfrac{ny}{R} - \frac{1}{2}\theta(y)\right] \end{pmatrix}. \end{aligned} \tag{19}$$

$\psi_R^{\langle n \rangle}$ and $\psi_L^{\langle n \rangle}$ combine to form the $\psi^{\langle n \rangle}(x)$ mode, whose mass is given by $m_n(\theta_H) = R^{-1}\left|n + \frac{\theta_H}{2\pi}\right|$. In the original gauge the KK expansion takes the form

$$\begin{aligned} \begin{pmatrix} u_R(x, y) \\ d_R(x, y) \end{pmatrix} &= \sum_{n=-\infty}^{\infty} \psi_R^{\langle n \rangle}(x) \frac{1}{\sqrt{\pi R}} \begin{pmatrix} \cos\dfrac{ny}{R} \\ \sin\dfrac{ny}{R} \end{pmatrix}, \\ \begin{pmatrix} u_L(x, y) \\ d_L(x, y) \end{pmatrix} &= \sum_{n=-\infty}^{\infty} \psi_L^{\langle n \rangle}(x) \frac{1}{\sqrt{\pi R}} \begin{pmatrix} \sin\dfrac{ny}{R} \\ -\cos\dfrac{ny}{R} \end{pmatrix}. \end{aligned} \tag{20}$$

The KK expansion for the fermion field Ψ' is found in a similar manner. The spectrum is determined, instead of Eq. (18), by

$$\sin^2 \lambda\pi R - \cos^2 \tfrac{1}{2}\theta_H = 0, \tag{21}$$

leading to the spectrum for λ: $\{R^{-1}(n + \frac{1}{2} \pm \theta_H/2\pi) \geq 0;\ n : \text{integers})\}$. The KK expansion becomes

$$\begin{aligned} \begin{pmatrix} u'_R(x, y) \\ d'_R(x, y) \end{pmatrix} &= \sum_{n=-\infty}^{\infty} \psi_R^{\prime\langle n+\frac{1}{2}\rangle}(x) \frac{1}{\sqrt{\pi R}} \begin{pmatrix} \cos\dfrac{(n+\frac{1}{2})y}{R} \\ \sin\dfrac{(n+\frac{1}{2})y}{R} \end{pmatrix}, \\ \begin{pmatrix} u'_L(x, y) \\ d'_L(x, y) \end{pmatrix} &= \sum_{n=-\infty}^{\infty} \psi_L^{\prime\langle n+\frac{1}{2}\rangle}(x) \frac{1}{\sqrt{\pi R}} \begin{pmatrix} \sin\dfrac{(n+\frac{1}{2})y}{R} \\ -\cos\dfrac{(n+\frac{1}{2})y}{R} \end{pmatrix}. \end{aligned} \tag{22}$$

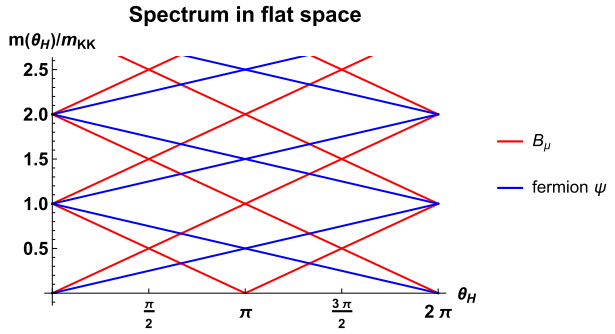

Fig. 1. The mass spectrum of gauge fields $B_\mu^{\langle n\rangle}$ and fermion fields $\psi^{\langle n\rangle}$ in flat $M^4 \times (S^1/Z_2)$ spacetime. Level crossings in the spectrum are seen.

$\psi_R^{\prime\langle n+\frac{1}{2}\rangle}$ and $\psi_L^{\prime\langle n+\frac{1}{2}\rangle}$ combine to form the $\psi^{\prime\langle n+\frac{1}{2}\rangle}(x)$ mode with mass $m_{n+\frac{1}{2}}(\theta_H) = R^{-1}\left|n+\frac{1}{2}+\frac{\theta_H}{2\pi}\right|$.

The spectrum of $B_\mu^{\langle n\rangle}$ and $\psi^{\langle n\rangle}$ modes is depicted in Fig. 1 in the range $0 \le \theta_H \le 2\pi$. The spectrum of $\psi^{\prime\langle n+\frac{1}{2}\rangle}$ modes is obtained from that of $\psi^{\langle n\rangle}$ modes by shifting θ_H by π. The KK mass scale is $m_{\rm KK} = 1/R$ in flat space. The spectrum of B_μ modes has periodicity with period π, whereas the spectrum of ψ and $\psi^{'}$ modes has periodicity with period 2π. In flat space the level crossing occurs at $\theta_H = 0, \frac{1}{2}\pi, \pi, \frac{3}{2}\pi$ for B_μ, and at $\theta_H = 0, \pi$ for ψ and $\psi^{'}$.

Next, we examine $SU(2)$ GHU in the RS space whose metric is given by [15]

$$ds^2 = e^{-2\sigma(y)}\eta_{\mu\nu}dx^\mu dx^\nu + dy^2, \tag{23}$$

where $\eta_{\mu\nu} = \mathrm{diag}(-1,+1,+1,+1)$, $\sigma(y) = \sigma(y+2L) = \sigma(-y)$, and $\sigma(y) = ky$ for $0 \le y \le L$. It has the same topology as $M^4 \times (S^1/Z_2)$. In the fundamental region $0 \le y \le L$ the metric can be written, in terms of the conformal coordinate $z = e^{ky}$, as

$$ds^2 = \frac{1}{z^2}\left(\eta_{\mu\nu}dx^\mu dx^\nu + \frac{dz^2}{k^2}\right) \qquad (1 \le z \le z_L = e^{kL}). \tag{24}$$

z_L is called the warp factor of the RS space. The action in RS is

$$\begin{aligned} I_{\rm RS} &= \int d^5x\sqrt{-\det G}\,\mathcal{L}_{\rm RS}, \\ \mathcal{L}_{\rm RS} &= -\frac{1}{2}\mathrm{Tr}\,F_{MN}F^{MN} + \overline{\Psi}\mathcal{D}(c)\Psi + \overline{\Psi}'\mathcal{D}(c')\Psi', \\ \mathcal{D}(c) &= \gamma^A e_A{}^M\left(D_M + \frac{1}{8}\omega_{MBC}[\gamma^B,\gamma^C]\right) - c\,k \qquad \text{for } 1 \le z \le z_L. \end{aligned} \tag{25}$$

Note that $\mathcal{L}_{\rm RS}(x^\mu, y) = \mathcal{L}_{\rm RS}(x^\mu, -y) = \mathcal{L}_{\rm RS}(x^\mu, y+2L)$. The fields A_M, Ψ, and $\Psi^{'}$ satisfy the same boundary conditions, Eq. (2), as in the flat space. The dimensionless bulk mass parameter c in $\mathcal{D}(c)$ controls the mass and wave function of the fermion fields. The KK mass scale is given by

$$m_{\rm KK} = \frac{\pi k}{z_L - 1}, \tag{26}$$

which becomes $1/R$ in the flat spacetime limit $k \to 0$.

In the KK expansion $A_z^a(x,z) = k^{-1/2}\sum A_z^{a(n)}(x)h_n(z)$, and the zero mode $A_z^{2(0)}$ has a wave function $h_0(z) = \sqrt{2/(z_L^2-1)}\,z$. In the y-coordinate $A_y^{2(0)}$ has a wave function $v_0(y) = ke^{ky}h_0(z)$

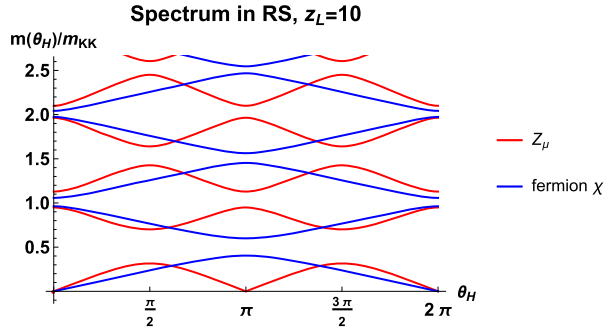

Fig. 2. The mass spectrum of gauge fields $Z_\mu^{(n)}$ and fermion fields $\chi^{(n)}$ in the RS warped space. The warp factor is $z_L = 10$, and the bulk mass parameter of Ψ is $c = 0.25$. There is no level crossing in the spectrum.

for $0 \le y \le L$, and $v_0(-y) = v_0(y) = v_0(y + 2L)$. The AB phase θ_H in Eq. (5) becomes

$$\theta_H = \frac{\langle A_z^{2(0)} \rangle}{f_H}, \qquad f_H = \frac{1}{g_4}\sqrt{\frac{2k}{L(z_L^2 - 1)}}. \tag{27}$$

The twisted gauge [13,14], in which $\tilde{\theta}_H = 0$, is related to the original gauge by a large gauge transformation:

$$\Omega(z) = e^{i\theta(z)\tau^2/2}, \qquad \theta(z) = \theta_H \frac{z_L^2 - z^2}{z_L^2 - 1}. \tag{28}$$

In the y-coordinate it is written as

$$\Omega(y) = \exp\left\{ i\theta_H \sqrt{\frac{2}{z_L^2 - 1}} \int_y^L dy\, v_0(y) \cdot \frac{\tau^2}{2} \right\}. \tag{29}$$

The boundary conditions in the twisted gauge are given by Eq. (7).

With the boundary conditions at $z = z_L$, eigenmodes of $\tilde{A}_\mu^1$ and $\tilde{A}_\mu^3$ are given in the form

$$\begin{pmatrix} \tilde{A}_\mu^1 \\ \tilde{A}_\mu^3 \end{pmatrix} = \begin{pmatrix} \alpha S(z;\lambda) \\ \beta C(z;\lambda) \end{pmatrix} Z_\mu^{(\lambda)}(x), \tag{30}$$

where $S(z;\lambda)$ and $C(z;\lambda)$ are expressed in terms of Bessel functions and are given by Eq. (A1). The boundary conditions at $z = 1$ lead to a condition obtained from Eq. (11) by substituting $S_\lambda(0)$, $C_\lambda(0)$, etc. by $S(1;\lambda)$, $C(1;\lambda)$, etc. As $(CS' - SC')(z;\lambda) = \lambda z$, the spectrum is determined by

$$SC'(1;\lambda_n) + \lambda_n \sin^2\theta_H = 0. \tag{31}$$

The corresponding mass is $m_n = k\lambda_n$. We label $\{\lambda_n\}$ from the bottom such that $\lambda_0(\theta_H) < \lambda_1(\theta_H) < \lambda_2(\theta_H) < \cdots$. There is no level crossing. The spectrum is periodic with period π, and is displayed in Fig. 2.

For a fermion field $\Psi(x, z)$ it is most convenient to express its KK expansion for $\check{\Psi}(x, z) = z^{-2}\Psi(x, z)$. Note that the Neumann boundary conditions at $z = (z_0, z_1) = (1, z_L)$, corresponding to even parity, for left- and right-handed components are given by

$$D_+(c)\check{\Psi}_L\big|_{z_j} = 0, \qquad D_-(c)\check{\Psi}_R\big|_{z_j} = 0, \qquad D_\pm(c) = \pm\frac{d}{dz} + \frac{c}{z}. \tag{32}$$

In the twisted gauge $\tilde{\tilde{\Psi}}$ satisfies free equations in the bulk. With the boundary conditions at $z = z_L$, the eigenmodes of $\check{\Psi}$ are written in the form

$$\begin{pmatrix} \tilde{\check{u}}_R \\ \tilde{\check{d}}_R \end{pmatrix}(x,z) = \begin{pmatrix} \alpha_R C_R(z;\lambda,c) \\ \beta_R S_R(z;\lambda,c) \end{pmatrix} f_{\lambda,R}(x), \quad \begin{pmatrix} \tilde{\check{u}}_L \\ \tilde{\check{d}}_L \end{pmatrix}(x,z) = \begin{pmatrix} \alpha_L S_L(z;\lambda,c) \\ \beta_L C_L(z;\lambda,c) \end{pmatrix} f_{\lambda,L}(x), \tag{33}$$

where the functions $C_{R/L}$ and $S_{R/L}$ are given in Eq. (A4). It follows from the equations of motion that $(\alpha_R, \beta_R) = (\alpha_L, \beta_L)$. The boundary conditions at $z = 1$, $D_-\check{u}_R = 0$ and $\check{d}_R = 0$, lead to

$$\begin{pmatrix} \bar{s}_H C_R(1) & \bar{c}_H S_R(1) \\ \bar{c}_H S_L(1) & -\bar{s}_H C_L(1) \end{pmatrix} \begin{pmatrix} \alpha_R \\ \beta_R \end{pmatrix} = 0, \tag{34}$$

where $C_R(1) = C_R(1;\lambda,c)$, etc., and the relation $D_-(c)(C_R, S_R) = \lambda(S_L, C_L)$ has been used. As $C_L C_R - S_L S_R = 1$, the spectrum is determined by

$$S_L S_R(1;\lambda_n,c) + \sin^2 \tfrac{1}{2}\theta_H = 0. \tag{35}$$

The corresponding mass is $m_n = k\lambda_n$. As in the case of the gauge field, we label $\{\lambda_n\}$ from the bottom such that $\lambda_0(\theta_H) < \lambda_1(\theta_H) < \lambda_2(\theta_H) < \cdots$. There is no level crossing. The spectrum is periodic with period 2π, and is displayed in Fig. 2.

Formulas for a fermion field Ψ' are obtained in a similar manner. With the boundary conditions at $z = z_L$, the eigenmodes of $\check{\Psi}'$ are written in the form of Eq. (33). The boundary conditions at $z = 1$ imply that $\check{u}'_R = 0$ and $D_-\check{d}'_R = 0$, so that the spectrum-determining equation becomes

$$S_L S_R(1;\lambda_n,c') + \cos^2 \tfrac{1}{2}\theta_H = 0. \tag{36}$$

Massless modes appear at $\theta_H = \pi$.

In Fig. 2 the mass spectrum of gauge fields $Z_\mu^{(n)}$ and fermion fields $\chi^{(n)}$ in RS is depicted. A distinct feature is that no level crossing occurs in the RS warped space. As the AB phase varies, the massless gauge fields $Z_\mu^{(0)}$ at $\theta_H = 0$ smoothly change to become massless gauge fields at $\theta_H = \pi$. The massless mode $\chi^{(0)}$ at $\theta_H = 0$, on the other hand, becomes massive at $\theta_H = \pi$. Chiral fermions are transformed to vector-like fermions by an AB phase. We confirm this in Sect. 4 by showing how gauge couplings change with θ_H. We also stress that the spectrum in the RS space in Fig. 2 converges to the spectrum in $M^4 \times (S^1/Z_2)$ in Fig. 1 in the limit $k \to 0$ ($z_L \to 1$).

3. Anomaly flow in $M^4 \times (S^1/Z_2)$

Four-dimensional gauge couplings of fermion fields in flat $M^4 \times (S^1/Z_2)$ spacetime are obtained by inserting the KK expansions for A_μ^a and Ψ into $-ig_A \int d^4x dy\, \bar{\Psi}\gamma^M A_M \Psi$ and integrating over y. It is most convenient to evaluate the couplings in the original gauge as the wave functions of KK modes do not depend on θ_H in the flat spacetime.

The spectrum and KK expansion of $A_\mu^2(x,y)$ are not affected by θ_H, and therefore

$$\begin{aligned} &-\frac{ig_A}{2}\int_0^L dy\, A_\mu^2 \left\{ u_R^\dagger \bar{\sigma}^\mu d_R - u_L^\dagger \sigma^\mu d_L - d_R^\dagger \bar{\sigma}^\mu u_R + d_L^\dagger \sigma^\mu u_L \right\} \\ &= -\frac{ig_4}{2\sqrt{2}} \sum_{n=1}^{\infty} A_\mu^{2(n)} \sum_{\ell=-\infty}^{\infty} \Big\{ \psi_R^{\langle\ell\rangle\,\dagger} \bar{\sigma}^\mu \psi_R^{\langle\ell+n\rangle} - \psi_R^{\langle\ell+n\rangle\,\dagger} \bar{\sigma}^\mu \psi_R^{\langle\ell\rangle} \\ &\quad - \psi_L^{\langle\ell\rangle\,\dagger} \sigma^\mu \psi_L^{\langle\ell+n\rangle} + \psi_L^{\langle\ell+n\rangle\,\dagger} \sigma^\mu \psi_L^{\langle\ell\rangle} \Big\}. \end{aligned} \tag{37}$$

Here, $\sigma^\mu = (I_2, \vec{\sigma})$ and $\bar{\sigma}^\mu = (-I_2, \vec{\sigma})$. All of the $A_\mu^{2(n)}$ couplings do not depend on θ_H in the above basis. Note that the zero modes $\psi_R^{\langle 0\rangle}$ and $\psi_L^{\langle 0\rangle}$ have chiral structure in Eq. (20).

The couplings of the $B_\mu^{\langle n\rangle}$ modes are evaluated similarly. By inserting the KK expansions in Eqs. (14) and (20), one finds

$$\begin{aligned}
&-\frac{ig_A}{2}\int_0^L dy\,\{A_\mu^1(\bar{u}\gamma^\mu d+\bar{d}\gamma^\mu u)+A_\mu^3(\bar{u}\gamma^\mu u-\bar{d}\gamma^\mu d)\}\\
&=\frac{g_4}{2}\sum_{n=-\infty}^{\infty}B_\mu^{\langle n\rangle}\sum_{\ell=-\infty}^{\infty}\left\{\psi_R^{\langle n-\ell\rangle\,\dagger}\bar{\sigma}^\mu\psi_R^{\langle\ell\rangle}+\psi_L^{\langle n-\ell\rangle\,\dagger}\sigma^\mu\psi_L^{\langle\ell\rangle}\right\}\\
&=\frac{g_4}{2}\sum_{n=-\infty}^{\infty}B_\mu^{\langle n\rangle}\sum_{\ell=-\infty}^{\infty}\bar{\psi}^{\langle n-\ell\rangle}\,i\gamma^5\gamma^\mu\psi^{\langle\ell\rangle}.
\end{aligned}\tag{38}$$

In the $B_\mu^{\langle n\rangle}$ basis the couplings $B_\mu^{\langle n\rangle}\psi_R^{\langle m\rangle\,\dagger}\psi_R^{\langle\ell\rangle}$ and $B_\mu^{\langle n\rangle}\psi_L^{\langle m\rangle\,\dagger}\psi_L^{\langle\ell\rangle}$ take a simple form: $\frac{1}{2}g_4\,\delta_{n,m+\ell}$.

At $\theta_H=0$ the $n=0$ mode of $B_\mu^{\langle n\rangle}$ is the massless gauge field of the unbroken $U(1)$. It has axial-vector couplings $\sum_{\ell=-\infty}^{\infty}\bar{\psi}^{\langle-\ell\rangle}\,i\gamma^5\gamma^\mu\psi^{\langle\ell\rangle}$. The coupling to the $\ell=0$ modes leads to a triangle chiral anomaly of three $B_\mu^{\langle0\rangle}$ legs with an anomaly coefficient $(g_4/2)^3(1+1)$, reflecting the chiral structure of $u_R^{(0)}$ and $d_L^{(0)}$. Note that off-diagonal couplings do not contribute to this anomaly. At $\theta_H=\pi$ the $B_\mu^{\langle-1\rangle}$ mode becomes the massless gauge field of the unbroken $U(1)$. It has axial-vector couplings $\sum_{\ell=-\infty}^{\infty}\bar{\psi}^{\langle-\ell-1\rangle}\,i\gamma^5\gamma^\mu\psi^{\langle\ell\rangle}$. No chiral anomaly arises associated with the three $B_\mu^{\langle-1\rangle}$ legs.

To investigate the structure of the anomalies let us write the B_μ couplings as

$$\frac{g_4}{2}\sum_{n=-\infty}^{\infty}\sum_{m=-\infty}^{\infty}\sum_{\ell=-\infty}^{\infty}B_\mu^{\langle n\rangle}\left\{s_{nm\ell}^R\,\psi_R^{\langle m\rangle\,\dagger}\bar{\sigma}^\mu\psi_R^{\langle\ell\rangle}+s_{nm\ell}^L\,\psi_L^{\langle m\rangle\,\dagger}\sigma^\mu\psi_L^{\langle\ell\rangle}\right\},\tag{39}$$

where, in the current case, $s_{nm\ell}^R=s_{nm\ell}^L=\delta_{n,m+\ell}$. The anomaly coefficients associated with the three legs of $B_{\mu_1}^{\langle n_1\rangle}B_{\mu_2}^{\langle n_2\rangle}B_{\mu_3}^{\langle n_3\rangle}$ are given by

$$\begin{aligned}
&b_{n_1n_2n_3}=b_{n_1n_2n_3}^R+b_{n_1n_2n_3}^L,\\
&b_{n_1n_2n_3}^R=\mathrm{Tr}\,S_{n_1}^RS_{n_2}^RS_{n_3}^R,\qquad \left(S_n^R\right)_{m\ell}=s_{nm\ell}^R,\\
&b_{n_1n_2n_3}^L=\mathrm{Tr}\,S_{n_1}^LS_{n_2}^LS_{n_3}^L,\qquad \left(S_n^L\right)_{m\ell}=s_{nm\ell}^L.
\end{aligned}\tag{40}$$

It follows that

$$b_{n_1n_2n_3}=\begin{cases}2 & \text{for } n_1+n_2+n_3=\text{even},\\ 0 & \text{for } n_1+n_2+n_3=\text{odd}.\end{cases}\tag{41}$$

Note that $b_{011},b_{200},b_{211},\ldots=2\neq0$. Anomalies arise even for massive KK excited gauge bosons in external legs. Triangle diagrams, for instance, in which fermions $\psi^{\langle0\rangle}$, $\psi^{\langle0\rangle}$, and $\psi^{\langle1\rangle}$ ($\psi^{\langle1\rangle}$, $\psi^{\langle1\rangle}$, and $\psi^{\langle-1\rangle}$) are running contribute to b_{011} (b_{200}) in perturbation theory. The divergence of the current $J_\mu^{\langle n\rangle}$ associated with $B_\mu^{\langle n\rangle}$ has anomalous terms proportional to $\sum_{m\ell}b_{nm\ell}\,\epsilon^{\mu\nu\rho\sigma}F_{\mu\nu}^{\langle m\rangle}F_{\rho\sigma}^{\langle\ell\rangle}$, where $F_{\mu\nu}^{\langle m\rangle}=\partial_\mu B_\nu^{\langle m\rangle}-\partial_\nu B_\mu^{\langle m\rangle}$.

In the B_μ basis $b_{n_1n_2n_3}$ is θ_H-independent. The anomaly does not seem to flow with θ_H in the flat space. However, the level crossing in the spectrum occurs in the flat space. The $B_\mu^{\langle0\rangle}$ mode corresponds to the lowest mode for $0\le\theta_H<\frac{1}{2}\pi$, but becomes the first excited KK mode for $\frac{1}{2}\pi<\theta_H<\pi$. In the RS space there is no level crossing. The lowest gauge field mode remains as the lowest mode for any value of θ_H. When the anti-de Sitter curvature of the RS space is very small, namely for $k\ll m_{\mathrm{KK}}$, the anomaly associated with the three legs of the lowest gauge field must approach b_{nnn} with $n=-1$ (namely zero) for $\frac{1}{2}\pi<\theta_H<\pi$. In other words the anomaly must flow from 2 to 0 as θ_H varies from 0 to π. We see in the next section how this happens.

The contributions of the Ψ' field to anomalies are evaluated in a similar manner. With the KK expansion in Eq. (22), the B_μ couplings are given by

$$\frac{g_4}{2}\sum_{n=-\infty}^{\infty}\sum_{m=-\infty}^{\infty}\sum_{\ell=-\infty}^{\infty} B_\mu^{\langle n\rangle}\left\{ s'^R_{nm\ell}\,\psi_R'^{\left\langle m+\frac{1}{2}\right\rangle\dagger}\bar\sigma^\mu\psi_R'^{\left\langle \ell+\frac{1}{2}\right\rangle} + s'^L_{nm\ell}\,\psi_L'^{\left\langle m+\frac{1}{2}\right\rangle\dagger}\sigma^\mu\psi_L'^{\left\langle \ell+\frac{1}{2}\right\rangle}\right\}, \tag{42}$$

where $s'^R_{nm\ell} = s'^L_{nm\ell} = \delta_{n,m+\ell+1}$. The anomaly coefficient associated with $B_{\mu_1}^{\langle n_1\rangle}B_{\mu_2}^{\langle n_2\rangle}B_{\mu_3}^{\langle n_3\rangle}$ is given by formulas similar to Eq. (40) where all the quantities are replaced by primed ones: $b_{nm\ell}\to b'_{nm\ell}$, $s^R_{nm\ell}\to s'^R_{nm\ell}$, etc. One sees that

$$b'_{n_1n_2n_3} = \begin{cases} 0 & \text{for } n_1+n_2+n_3 = \text{even},\\ 2 & \text{for } n_1+n_2+n_3 = \text{odd}. \end{cases} \tag{43}$$

4. Anomaly flow in RS

The KK expansion of the gauge fields $A_\mu^{1,3}$ becomes

$$\begin{pmatrix}\tilde A_\mu^1(x,z)\\ \tilde A_\mu^3(x,z)\end{pmatrix} = \sqrt{k}\sum_{n=0}^{\infty} Z_\mu^{(n)}(x)\,\mathbf{h}_n(z), \tag{44}$$

where the mode functions are given by

$$\mathbf{h}_0(z) = \bar{\mathbf{h}}_0^a(z);$$

$$\mathbf{h}_{2\ell-1}(z) = (-1)^\ell\begin{cases} \bar{\mathbf{h}}^a_{2\ell-1}(z) & \text{for } -\frac{1}{2}\pi < \theta_H < \frac{1}{2}\pi,\\ \bar{\mathbf{h}}^b_{2\ell-1}(z) & \text{for } 0 < \theta_H < \pi,\\ -\bar{\mathbf{h}}^a_{2\ell-1}(z) & \text{for } \frac{1}{2}\pi < \theta_H < \frac{3}{2}\pi,\\ -\bar{\mathbf{h}}^b_{2\ell-1}(z) & \text{for } \pi < \theta_H < 2\pi,\\ \bar{\mathbf{h}}^a_{2\ell-1}(z) & \text{for } \frac{3}{2}\pi < \theta_H < \frac{5}{2}\pi \end{cases} \qquad (\ell = 1,2,3,\ldots);$$

$$\mathbf{h}_{2\ell}(z) = (-1)^\ell\begin{cases} \bar{\mathbf{h}}^b_{2\ell}(z) & \text{for } -\frac{1}{2}\pi < \theta_H < \frac{1}{2}\pi,\\ -\bar{\mathbf{h}}^a_{2\ell}(z) & \text{for } 0 < \theta_H < \pi,\\ -\bar{\mathbf{h}}^b_{2\ell}(z) & \text{for } \frac{1}{2}\pi < \theta_H < \frac{3}{2}\pi,\\ \bar{\mathbf{h}}^a_{2\ell}(z) & \text{for } \pi < \theta_H < 2\pi,\\ \bar{\mathbf{h}}^b_{2\ell}(z) & \text{for } \frac{3}{2}\pi < \theta_H < \frac{5}{2}\pi \end{cases} \qquad (\ell = 1,2,3,\ldots). \tag{45}$$

Here,

$$\bar{\mathbf{h}}_n^a(z) = \frac{1}{\sqrt{r_n^a}}\begin{pmatrix}-s_H\hat S(z;\lambda_n)\\ c_H C(z;\lambda_n)\end{pmatrix},$$
$$\bar{\mathbf{h}}_n^b(z) = \frac{1}{\sqrt{r_n^b}}\begin{pmatrix}c_H S(z;\lambda_n)\\ s_H\check C(z;\lambda_n)\end{pmatrix},$$
$$r_n = \int_1^{z_L}\frac{dz}{z}\left\{|h_n(z)|^2 + |k_n(z)|^2\right\} \qquad \text{for } \begin{pmatrix}h_n(z)\\ k_n(z)\end{pmatrix}. \tag{46}$$

$\hat S$ and $\check C$ are given in Eq. (A3). The spectrum-determining equation, Eq. (31), can be written as $C\hat S'(1;\lambda_n) - \lambda_n\cos^2\theta_H = 0$. At $\theta_H = 0$ and π, $S(1;\lambda_n) = 0$ for even n and $C'(1;\lambda_n) = 0$ for odd n. At $\theta_H = \frac{1}{2}\pi$ and $\frac{3}{2}\pi$, $S'(1;\lambda_n) = 0$ for even n and $C(1;\lambda_n) = 0$ for odd n. This is why the connection formulas are necessary in Eq. (45). The expression $\bar{\mathbf{h}}^a_{2\ell-1}(z)$, for instance, fails to make sense at $\theta_H = \frac{1}{2}\pi$ as both $\hat S(z;\lambda_{2\ell-1})$ and c_H vanish there. In deriving the connection

formulas, we have made use of the identity

$$\begin{pmatrix} s_H \hat{S}(z;\lambda_n) \\ -c_H C(z;\lambda_n) \end{pmatrix} = K \begin{pmatrix} c_H S(z;\lambda_n) \\ s_H \check{C}(z;\lambda_n) \end{pmatrix}, \qquad K = \frac{s_H C(1;\lambda_n)}{c_H S(1;\lambda_n)} = -\frac{c_H C'(1;\lambda_n)}{s_H S'(1;\lambda_n)}, \tag{47}$$

valid at $|\theta_H| \neq 0, \frac{1}{2}\pi, \pi, \ldots$ As a consequence, $\bar{\mathbf{h}}^a_{2\ell-1}(z) = \bar{\mathbf{h}}^b_{2\ell-1}(z)$ for $0 < \theta_H < \frac{1}{2}\pi$ and $\bar{\mathbf{h}}^a_{2\ell-1}(z) = -\bar{\mathbf{h}}^b_{2\ell-1}(z)$ for $\frac{1}{2}\pi < \theta_H < \pi$ in Eq. (45). In the numerical evaluation of anomalies we have used, for instance, $\mathbf{h}_{2\ell-1}(z) = (-1)^\ell \bar{\mathbf{h}}^a_{2\ell-1}(z)$ for $-\frac{1}{4}\pi < \theta_H \leq \frac{1}{4}\pi$, $(-1)^\ell \bar{\mathbf{h}}^b_{2\ell-1}(z)$ for $\frac{1}{4}\pi < \theta_H \leq \frac{3}{4}\pi$, and so on. $\mathbf{h}_0(z)$ is periodic in θ_H with period 2π, whereas all other modes $\mathbf{h}_n(z)$ $(n \geq 1)$ have period π.

The mode functions of the fermion field Ψ are found in a similar manner. In the KK expansions

$$\begin{pmatrix} \tilde{\tilde{u}}_R(x,z) \\ \tilde{\tilde{d}}_R(x,z) \end{pmatrix} = \sqrt{k} \sum_{n=0}^{\infty} \chi_R^{(n)}(x) \mathbf{f}_{Rn}(z), \qquad \begin{pmatrix} \tilde{\tilde{u}}_L(x,z) \\ \tilde{\tilde{d}}_L(x,z) \end{pmatrix} = \sqrt{k} \sum_{n=0}^{\infty} \chi_L^{(n)}(x) \mathbf{f}_{Ln}(z) \tag{48}$$

the mode functions are given, for $c > 0$, by

$$\mathbf{f}_{R,2\ell}(z) = \begin{cases} \bar{\mathbf{f}}^a_{R,2\ell}(z) & \text{for } -\pi < \theta_H < \pi, \\ \bar{\mathbf{f}}^b_{R,2\ell}(z) & \text{for } 0 < \theta_H < 2\pi, \\ -\bar{\mathbf{f}}^a_{R,2\ell}(z) & \text{for } \pi < \theta_H < 3\pi, \\ -\bar{\mathbf{f}}^b_{R,2\ell}(z) & \text{for } 2\pi < \theta_H < 4\pi, \\ \bar{\mathbf{f}}^a_{R,2\ell}(z) & \text{for } 3\pi < \theta_H < 5\pi \end{cases} \qquad (\ell = 0, 1, 2, \ldots);$$

$$\mathbf{f}_{R,2\ell-1}(z) = \begin{cases} \bar{\mathbf{f}}^c_{R,2\ell-1}(z) & \text{for } -\pi < \theta_H < \pi, \\ \bar{\mathbf{f}}^d_{R,2\ell-1}(z) & \text{for } 0 < \theta_H < 2\pi, \\ -\bar{\mathbf{f}}^c_{R,2\ell-1}(z) & \text{for } \pi < \theta_H < 3\pi, \\ -\bar{\mathbf{f}}^d_{R,2\ell-1}(z) & \text{for } 2\pi < \theta_H < 4\pi, \\ \bar{\mathbf{f}}^c_{R,2\ell-1}(z) & \text{for } 3\pi < \theta_H < 5\pi \end{cases} \qquad (\ell = 1, 2, 3, \ldots) \tag{49}$$

and

$$\mathbf{f}_{L0}(z) = \bar{\mathbf{f}}^a_{L0}(z);$$

$$\mathbf{f}_{L,2\ell-1}(z) = \begin{cases} \bar{\mathbf{f}}^a_{L,2\ell-1}(z) & \text{for } -\pi < \theta_H < \pi, \\ \bar{\mathbf{f}}^b_{L,2\ell-1}(z) & \text{for } 0 < \theta_H < 2\pi, \\ -\bar{\mathbf{f}}^a_{L,2\ell-1}(z) & \text{for } \pi < \theta_H < 3\pi, \\ -\bar{\mathbf{f}}^b_{L,2\ell-1}(z) & \text{for } 2\pi < \theta_H < 4\pi, \\ \bar{\mathbf{f}}^a_{L,2\ell-1}(z) & \text{for } 3\pi < \theta_H < 5\pi \end{cases} \qquad (\ell = 1, 2, 3, \ldots);$$

$$\mathbf{f}_{L,2\ell}(z) = \begin{cases} \bar{\mathbf{f}}^c_{L,2\ell}(z) & \text{for } -\pi < \theta_H < \pi, \\ \bar{\mathbf{f}}^d_{L,2\ell}(z) & \text{for } 0 < \theta_H < 2\pi, \\ -\bar{\mathbf{f}}^c_{L,2\ell}(z) & \text{for } \pi < \theta_H < 3\pi, \\ -\bar{\mathbf{f}}^d_{L,2\ell}(z) & \text{for } 2\pi < \theta_H < 4\pi, \\ \bar{\mathbf{f}}^c_{L,2\ell}(z) & \text{for } 3\pi < \theta_H < 5\pi \end{cases} \qquad (\ell = 1, 2, 3, \ldots). \tag{50}$$

Here,

$$\bar{\mathbf{f}}^a_{Rn}(z) = \frac{1}{\sqrt{r^a_n}}\begin{pmatrix} \bar{c}_H C_R(z;\lambda_n,c) \\ -\bar{s}_H \hat{S}_R(z;\lambda_n,c)\end{pmatrix}, \qquad \bar{\mathbf{f}}^b_{Rn}(z) = \frac{1}{\sqrt{r^b_n}}\begin{pmatrix} \bar{s}_H C_R(z;\lambda_n,c) \\ \bar{c}_H \check{S}_R(z;\lambda_n,c)\end{pmatrix},$$

$$\bar{\mathbf{f}}^c_{Rn}(z) = \frac{1}{\sqrt{r^c_n}}\begin{pmatrix} \bar{s}_H \hat{C}_R(z;\lambda_n,c) \\ \bar{c}_H S_R(z;\lambda_n,c)\end{pmatrix}, \qquad \bar{\mathbf{f}}^d_{Rn}(z) = \frac{1}{\sqrt{r^d_n}}\begin{pmatrix} -\bar{c}_H \check{C}_R(z;\lambda_n,c) \\ \bar{s}_H S_R(z;\lambda_n,c)\end{pmatrix},$$

$$\bar{\mathbf{f}}^a_{Ln}(z) = \frac{1}{\sqrt{r^a_n}}\begin{pmatrix} \bar{s}_H \hat{S}_L(z;\lambda_n,c) \\ \bar{c}_H C_L(z;\lambda_n,c)\end{pmatrix}, \qquad \bar{\mathbf{f}}^b_{Ln}(z) = \frac{1}{\sqrt{r^b_n}}\begin{pmatrix} -\bar{c}_H \check{S}_L(z;\lambda_n,c) \\ \bar{s}_H C_L(z;\lambda_n,c)\end{pmatrix},$$

$$\bar{\mathbf{f}}^c_{Ln}(z) = \frac{1}{\sqrt{r^c_n}}\begin{pmatrix} \bar{c}_H S_L(z;\lambda_n,c) \\ -\bar{s}_H \hat{C}_L(z;\lambda_n,c)\end{pmatrix}, \qquad \bar{\mathbf{f}}^d_{Ln}(z) = \frac{1}{\sqrt{r^d_n}}\begin{pmatrix} \bar{s}_H S_L(z;\lambda_n,c) \\ \bar{c}_H \check{C}_L(z;\lambda_n,c)\end{pmatrix}, \tag{51}$$

$$\text{where } r_n = \int_1^{z_L} dz\{|f_n(z)|^2 + |g_n(z)|^2\} \qquad \text{for } \begin{pmatrix} f_n(z) \\ g_n(z)\end{pmatrix}. \tag{52}$$

The functions $\hat{S}_{R/L}$, $\check{S}_{R/L}$, etc. are defined in Eq. (A6). At $\theta_H = 0$ the $n = 0$ mode is massless: $\lambda_0 = 0$. Its wave function has chiral structure. $\chi^{(0)}_R$ is u-type, whereas $\chi^{(0)}_L$ is d-type. We show below that the $n = 0$ mode becomes vector-like as θ_H varies to π. At $\theta_H = 0$, $S_L(1;\lambda_n,c) = 0$ for even n whereas $S_R(1;\lambda_n,c) = 0$ for odd n. At $\theta_H = \pi$, $C_R(1;\lambda_n,c) = 0$ for even n whereas $C_L(1;\lambda_n,c) = 0$ for odd n. This is why the connection formulas are necessary in Eqs. (49) and (50). The wave function of the $\chi^{(0)}_L$ mode, $\mathbf{f}_{L0}(z)$, is periodic in θ_H with period 4π. The wave functions of all the other modes are periodic in θ_H with period 2π. The wave functions for $c < 0$ are tabulated in Appendix B.

The four-dimensional part of the gauge interactions for the Ψ field is given by

$$g_A \int d^4x \int_1^{z_L} \frac{dz}{k}\left\{\tilde{\tilde{\Psi}}^\dagger_R \bar{\sigma}^\mu \tilde{A}_\mu \tilde{\tilde{\Psi}}_R - \tilde{\tilde{\Psi}}^\dagger_L \sigma^\mu \tilde{A}_\mu \tilde{\tilde{\Psi}}_L\right\}. \tag{53}$$

To find the $Z^{(n)}_\mu$ couplings of the fermion modes, we write

$$\mathbf{h}_n(z) = \begin{pmatrix} h_n(z) \\ k_n(z)\end{pmatrix}, \qquad \mathbf{f}_{Rn}(z) = \begin{pmatrix} f_{Rn}(z) \\ g_{Rn}(z)\end{pmatrix}, \qquad \mathbf{f}_{Ln}(z) = \begin{pmatrix} f_{Ln}(z) \\ g_{Ln}(z)\end{pmatrix}. \tag{54}$$

By inserting the KK expansions in Eqs. (44) and (48) into Eq. (53), the $Z^{(n)}_\mu$ couplings of the χ_n fields are found to be

$$\frac{g_4}{2}\sum_{n=0}^{\infty}\sum_{\ell=0}^{\infty}\sum_{m=0}^{\infty} Z^{(n)}_\mu(x)\left\{t^R_{n\ell m}\,\chi^{(\ell)}_R(x)^\dagger \bar{\sigma}^\mu \chi^{(m)}_R(x) + t^L_{n\ell m}\,\chi^{(\ell)}_L(x)^\dagger \sigma^\mu \chi^{(m)}_L(x)\right\},$$

$$t^R_{n\ell m} = \sqrt{kL}\int_1^{z_L} dz\left\{h_n(z)\big(f^*_{R\ell}(z) g_{Rm}(z) + g^*_{R\ell}(z) f_{Rm}(z)\big)\right.$$
$$\left. + k_n(z)\big(f^*_{R\ell}(z) f_{Rm}(z) - g^*_{R\ell}(z) g_{Rm}(z)\big)\right\},$$

$$t^L_{n\ell m} = -\sqrt{kL}\int_1^{z_L} dz\left\{h_n(z)\big(f^*_{L\ell}(z) g_{Lm}(z) + g^*_{L\ell}(z) f_{Lm}(z)\big)\right.$$
$$\left. + k_n(z)\big(f^*_{L\ell}(z) f_{Lm}(z) - g^*_{L\ell}(z) g_{Lm}(z)\big)\right\}. \tag{55}$$

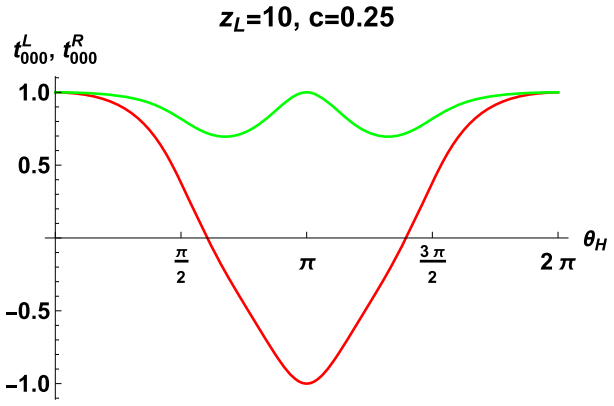

Fig. 3. The coupling constants $t^R_{000}(\theta_H)$ (red) and $t^L_{000}(\theta_H)$ (green) in Eq. (55) for the warp factor $z_L = 10$ and the bulk mass parameter $c = 0.25$.

The anomaly coefficient associated with the three legs of $Z^{(n_1)}_{\mu_1} Z^{(n_2)}_{\mu_2} Z^{(n_3)}_{\mu_3}$ is given by

$$\begin{aligned} a_{n_1n_2n_3} &= a^R_{n_1n_2n_3} + a^L_{n_1n_2n_3}, \\ a^R_{n_1n_2n_3} &= \mathrm{Tr}\, T^R_{n_1} T^R_{n_2} T^R_{n_3}, \qquad \left(T^R_n\right)_{m\ell} = t^R_{nm\ell}, \\ a^L_{n_1n_2n_3} &= \mathrm{Tr}\, T^L_{n_1} T^L_{n_2} T^L_{n_3}, \qquad \left(T^L_n\right)_{m\ell} = t^L_{nm\ell}. \end{aligned} \tag{56}$$

Unlike $s^{R/L}_{nm\ell}$ in the flat space, $t^{R/L}_{nm\ell}$ is θ_H-dependent. The anomaly coefficient $a_{n_1n_2n_3}$ also becomes θ_H-dependent, exhibiting the anomaly flow.

Let us first examine $a_{000}(\theta_H)$ at $\theta_H = 0$ and π, where the gauge field $Z^{(0)}_\mu$ becomes massless. At $\theta_H = 0$, $h_0(z) = 0$ and $k_0(z) = 1/\sqrt{kL}$. The fermion zero mode is chiral, g_{L0}, $f_{R0} \neq 0$ and $g_{R0} = f_{L0} = 0$. All the other modes are vector-like: $f_{R\,2\ell-1} = f_{L\,2\ell-1} = g_{R\,2\ell} = g_{L\,2\ell} = 0$ for $\ell = 1, 2, 3, \ldots$ It follows from the orthonormality conditions that $t^R_{0m\ell}$, $t^L_{0m\ell} = 0$ for $m \neq \ell$. It is seen that $t^R_{000} = t^L_{000} = 1$ and $t^R_{0nn} = -t^L_{0nn} = (-1)^n$ for $n \geq 1$. Hence, $a_{000}(0) = 2$, which is the same value as $b_{000}(0) = 2$ in the flat space.

At $\theta_H = \pi$, $h_0(z) = 0$ and $k_0(z) = -1/\sqrt{kL}$. All of the fermion modes are vector-like: $g_{R\,2\ell} = g_{L\,2\ell} = f_{R\,2\ell+1} = f_{L\,2\ell+1} = 0$ for $\ell = 0, 1, 2, \ldots$ Further, $t^R_{0m\ell}$, $t^L_{0m\ell} = 0$ for $m \neq \ell$, and $-t^R_{0nn} = t^L_{0nn} = (-1)^n$ for $n \geq 0$. It follows that $a_{000}(\pi) = 0$, which agrees with $b_{-1,\,-1,\,-1}(\pi) = 0$ in the flat space.

The θ_H-dependence of the coupling constants t^R_{000}, t^L_{000} and anomaly coefficients a_{000}, a^R_{000}, a^L_{000} is displayed in Figs. 3 and 4 for $z_L = 10$ and $c = 0.25$. All of them change smoothly as θ_H. The coupling constants of the fermion zero modes are maximally chiral at $\theta_H = 0$, but become purely vector-like at $\theta_H = \pi$. The anomaly is exactly cancelled among the right-handed and left-handed components at $\theta_H = \pi$. We note that, for the anomaly coefficient $a_{n_1n_2n_3}$, off-diagonal gauge couplings $t^{R/L}_{nm\ell}$ also contribute in Eq. (56). In the previous section we saw that, in the flat space, off-diagonal gauge couplings $s^{R/L}_{nm\ell} = \delta_{n,m+\ell}$ are important to $b_{n_1n_2n_3}$. In the RS space the couplings $t^{R/L}_{nm\ell}(\theta_H)$ are more involved, giving rise to the nontrivial θ_H-dependence of $a_{nm\ell}$.

Anomalies appear for various combinations of external gauge fields. In Fig. 5 the anomalies a_{111}, a_{222}, a_{001}, and a_{002} are displayed. In the RS space the gauge couplings of the first excited gauge boson $Z^{(1)}_\mu$ to fermions become larger. The anomaly coefficients associated with $Z^{(1)}_\mu$ become larger as the warp factor z_L increases. Each coefficient has nontrivial θ_H-dependence.

The anomaly coefficient $a_{n_1n_2n_3}(\theta_H)$ depends on both the warp factor z_L and the bulk mass parameter c. The couplings t^R_{000} and t^L_{000} and the anomaly coefficients a_{000}, a^R_{000}, and a^L_{000} for

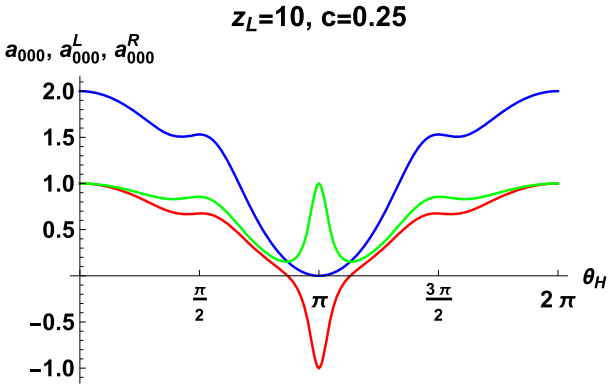

Fig. 4. The anomaly coefficients $a_{000}(\theta_H)$ (blue), $a^R_{000}(\theta_H)$ (red), and $a^L_{000}(\theta_H)$ (green) in Eq. (56) for the warp factor $z_L = 10$ and the bulk mass parameter $c = 0.25$.

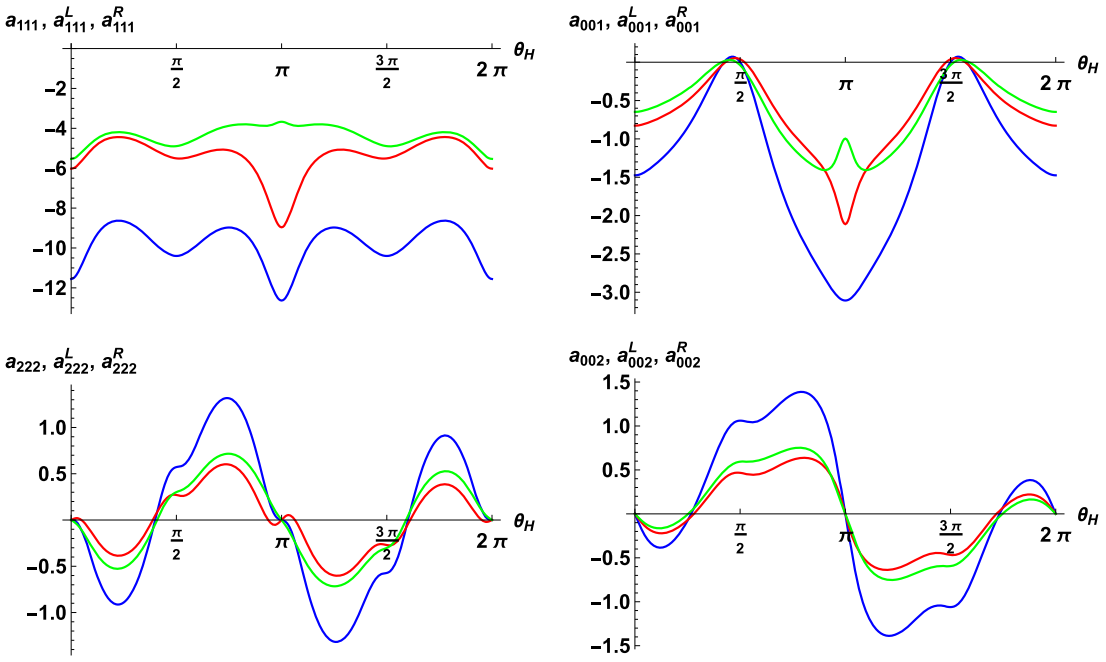

Fig. 5. The anomaly coefficients $a_{111}(\theta_H)$, $a_{001}(\theta_H)$, $a_{222}(\theta_H)$, and $a_{002}(\theta_H)$ in Eq. (56) are displayed for the warp factor $z_L = 10$ and the bulk mass parameter $c = 0.25$. The blue, red, and green lines correspond to $a_{n\ell m}$, $a^R_{n\ell m}$, and $a^L_{n\ell m}$, respectively.

$c = 0.8$ and $z_L = 10$ are displayed in Fig. 6. The couplings of right- and left-handed fermions exhibit large c-dependence. It is seen, however, that the total anomaly coefficient $a_{000}(\theta_H)$ is independent of c, being universal. In the numerical evaluation of anomalies we have incorporated the contributions of fermions $\chi^{(n)}$ ($n = 0, \ldots, n_{\max}$). In Fig. 7, $\Delta a_{000}(\theta_H) = a_{000}(\theta_H)_{c=0.25} - a_{000}(\theta_H)_{c=0.8}$ is plotted with $n_{\max} = 6$, 10, and 14 for $z_L = 10$. As $n_{\max}$ is increased, the difference $\Delta a_{000}(\theta_H)$ diminishes, approaching zero. The maximum of $|\Delta a_{000}(\theta_H)|$ is about 0.000 153 at $\theta_H = \frac{7}{20}\pi$ and $\frac{33}{20}\pi$ for $n_{\max} = 14$. It is expected that $a_{000}(\theta_H)$ becomes c-independent in the $n_{\max} \to \infty$ limit. We stress that the c-independence of $a_{n\ell m}(\theta_H)$ is highly nontrivial as the gauge couplings $t^{R/L}_{n\ell m}$ depend on c.

For negative c the roles of left- and right-handed fermions are interchanged. In other words, $t^R_{n\ell m}|_{-c} = t^L_{n\ell m}|_c$ and $a^R_{n\ell m}|_{-c} = a^L_{n\ell m}|_c$, and therefore $a_{n\ell m}(\theta_H)_{-c} = a_{n\ell m}(\theta_H)_c$.

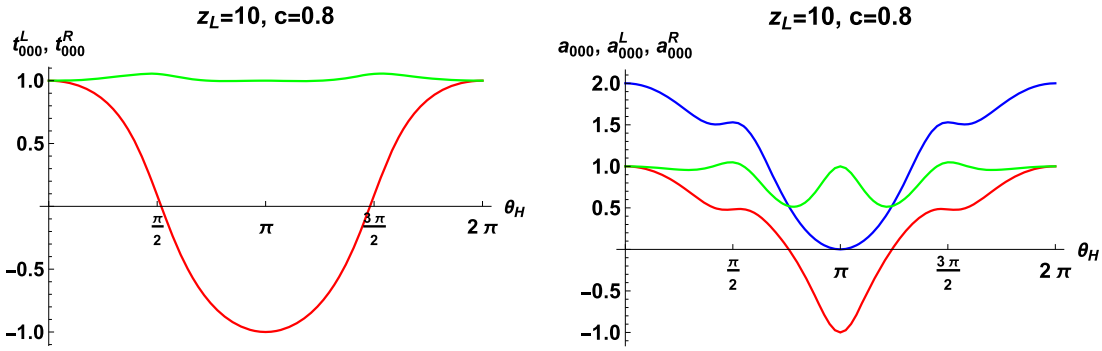

Fig. 6. Left: The couplings t^L_{000} (green) and t^R_{000} (red). Right: The anomaly coefficients a_{000} (blue), a^L_{000} (green), and a^R_{000} (red). Both plots are for $z_L = 10$ and $c = 0.8$. $a_{000}(\theta_H)$ shows little dependence on c.

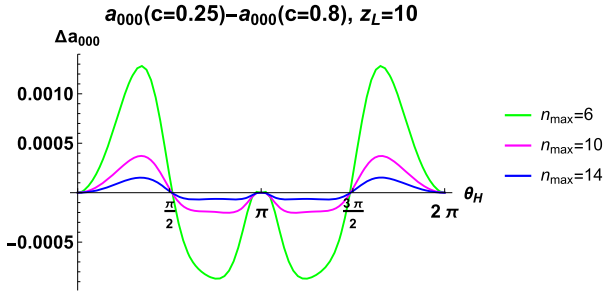

Fig. 7. The dependence of the anomaly coefficient $a_{000}(\theta_H)$ on the bulk mass parameter c. $a_{000}(\theta_H)_{c=0.25} - a_{000}(\theta_H)_{c=0.8}$ for $z_L = 10$ evaluated by taking account of fermion modes $\chi^{(n)}$ ($n = 0, \ldots, n_{\max}$) for $n_{\max} = 6$ (green), 10 (magenta), and 14 (blue). The result indicates that $a_{000}(\theta_H)$ becomes c-independent as $n_{\max} \to \infty$.

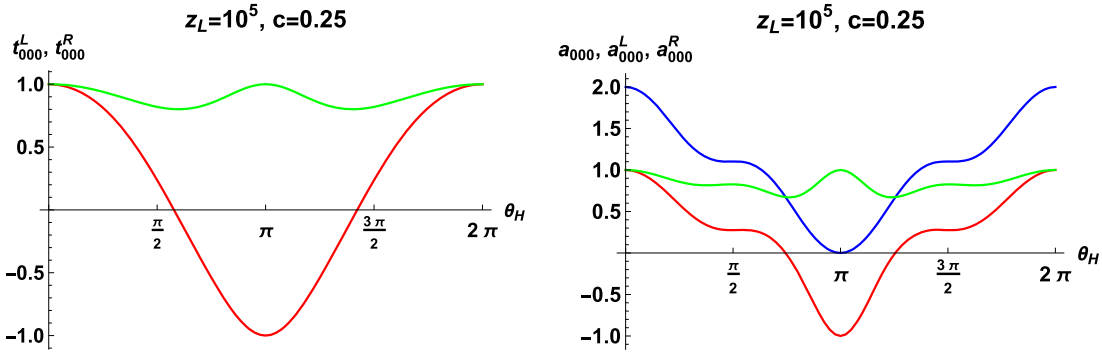

Fig. 8. Left: The couplings t^L_{000} (green) and t^R_{000} (red). Right: The anomaly coefficients a_{000} (blue), a^L_{000} (green) and a^R_{000} (red). Both plots are for $z_L = 10^5$ and $c = 0.25$.

The z_L-dependence is investigated similarly. For large $z_L = e^{kL} \gg 1$ the qualitative behavior does not change very much. In Fig. 8 the couplings t^R_{000} and t^L_{000} and the anomaly coefficients a_{000}, a^R_{000} and a^L_{000} for $z_L = 10^5$ and $c = 0.25$ are displayed. Compared to the case of $z_L = 10$ and $c = 0.25$, the behavior of the anomaly coefficients becomes milder.

The flat space limit, $k/m_{\rm KK} = (z_L - 1)/\pi \to 0$, exhibits singular behavior. In the flat space, $M^4 \times (S^1/Z_2)$, anomaly coefficients $b_{n\ell m}(\theta_H)$ are constant. It implies that except at the points of level crossings, $\theta_H = 0, \pm\frac{1}{2}\pi, \pm\pi$, $a_{n\ell m}$ must approach to a constant value in the flat space limit, and therefore must show step-function type behavior. In Fig. 9 the anomaly coefficients

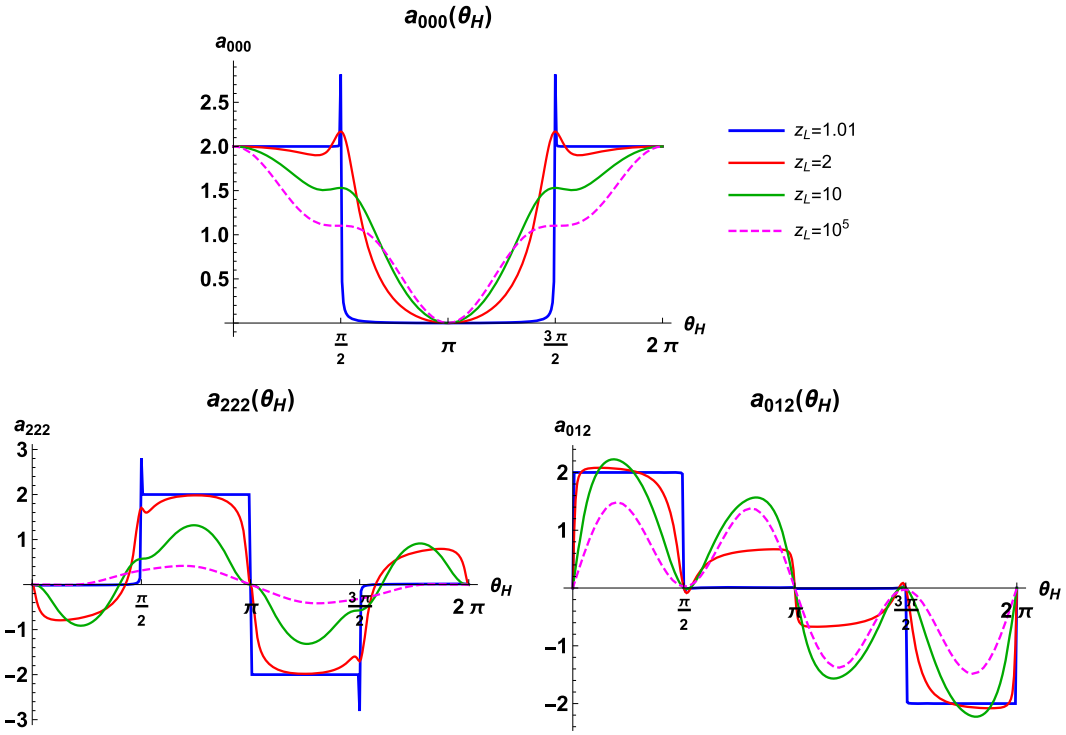

Fig. 9. The anomaly coefficients $a_{000}(\theta_H)$, $a_{222}(\theta_H)$, and $a_{012}(\theta_H)$ with $c = 0.25$ for $z_L = 1.01$, 2, 10, and 10^5. The flat space limit corresponds to $k \to 0$ and $z_L \to 1$.

Table 1. The correspondence between $B_\mu^{\langle n\rangle}$ and $Z_\mu^{(n)}$ in the flat space limit.

θ_H	$Z^{(0)}$	$Z^{(1)}$	$Z^{(2)}$	$Z^{(3)}$
0	$B^{\langle 0\rangle}$	$\frac{1}{\sqrt{2}}(B^{\langle 1\rangle}+B^{\langle -1\rangle})$	$\frac{1}{\sqrt{2}}(B^{\langle 1\rangle}-B^{\langle -1\rangle})$	$\frac{1}{\sqrt{2}}(B^{\langle 2\rangle}+B^{\langle -2\rangle})$
$(0,\frac{1}{2}\pi)$	$B^{\langle 0\rangle}$	$B^{\langle -1\rangle}$	$B^{\langle 1\rangle}$	$B^{\langle -2\rangle}$
$\frac{1}{2}\pi$	$\frac{1}{\sqrt{2}}(B^{\langle -1\rangle}+B^{\langle 0\rangle})$	$\frac{1}{\sqrt{2}}(B^{\langle -1\rangle}-B^{\langle 0\rangle})$	$\frac{1}{\sqrt{2}}(B^{\langle -2\rangle}+B^{\langle 1\rangle})$	$\frac{1}{\sqrt{2}}(B^{\langle -2\rangle}-B^{\langle 1\rangle})$
$(\frac{1}{2}\pi,\pi)$	$B^{\langle -1\rangle}$	$-B^{\langle 0\rangle}$	$B^{\langle -2\rangle}$	$-B^{\langle 1\rangle}$
π	$B^{\langle -1\rangle}$	$\frac{-1}{\sqrt{2}}(B^{\langle -2\rangle}+B^{\langle 0\rangle})$	$\frac{1}{\sqrt{2}}(B^{\langle -2\rangle}-B^{\langle 0\rangle})$	$\frac{-1}{\sqrt{2}}(B^{\langle -3\rangle}+B^{\langle 1\rangle})$
$(\pi,\frac{3}{2}\pi)$	$B^{\langle -1\rangle}$	$-B^{\langle -2\rangle}$	$-B^{\langle 0\rangle}$	$-B^{\langle -3\rangle}$
$\frac{3}{2}\pi$	$\frac{1}{\sqrt{2}}(B^{\langle -1\rangle}+B^{\langle -2\rangle})$	$\frac{1}{\sqrt{2}}(B^{\langle -1\rangle}-B^{\langle -2\rangle})$	$\frac{-1}{\sqrt{2}}(B^{\langle 0\rangle}+B^{\langle -3\rangle})$	$\frac{1}{\sqrt{2}}(B^{\langle 0\rangle}-B^{\langle -3\rangle})$
$(\frac{3}{2}\pi,2\pi)$	$B^{\langle -2\rangle}$	$B^{\langle -1\rangle}$	$-B^{\langle -3\rangle}$	$B^{\langle 0\rangle}$
2π	$B^{\langle -2\rangle}$	$\frac{1}{\sqrt{2}}(B^{\langle -1\rangle}+B^{\langle -3\rangle})$	$\frac{1}{\sqrt{2}}(B^{\langle -1\rangle}-B^{\langle -3\rangle})$	$\frac{1}{\sqrt{2}}(B^{\langle 0\rangle}+B^{\langle -4\rangle})$
$(2\pi,\frac{5}{2}\pi)$	$B^{\langle -2\rangle}$	$B^{\langle -3\rangle}$	$B^{\langle -1\rangle}$	$B^{\langle -4\rangle}$

$a_{000}(\theta_H)$, $a_{222}(\theta_H)$ and $a_{012}(\theta_H)$ with $c = 0.25$ are plotted for various values of z_L. It is seen that all of them approach to step functions with singularities at $\theta_H = 0, \frac{1}{2}\pi, \pi$ or $\frac{3}{2}\pi$ as $z_L \to 1$.

At this juncture it is appropriate to look at the correspondence between $B_\mu^{\langle n\rangle}$ and $Z_\mu^{(n)}$ in the flat space limit, which can be found from the mass spectra displayed in Figs. 1 and 2, the mode functions of $B_\mu^{\langle n\rangle}$ in Eq. (13), and the mode functions of $Z_\mu^{(n)}$ in Eq. (45). The results for $Z_\mu^{(n)}$ ($n = 0, 1, 2, 3$) are tabulated in Table 1. Using the relationships in Table 1, the anomaly coefficients

Table 2. The anomaly coefficients $a_{n\ell m}(\theta_H)$ due to the Ψ field in the flat space limit. Singular behavior is observed at $\theta_H = 0$, $\frac{1}{2}\pi$, π, and $\frac{3}{2}\pi$.

θ_H	a_{000}	a_{111}	a_{222}	a_{001}	a_{011}	a_{002}	a_{022}	a_{012}
0	2	0	0	0	4	0	0	0
$\left(0, \frac{1}{2}\pi\right)$	2	0	0	0	2	0	2	2
$\frac{1}{2}\pi$	$2\sqrt{2}$	$-2\sqrt{2}$	$2\sqrt{2}$	0	0	$2\sqrt{2}$	$2\sqrt{2}$	0
$\left(\frac{1}{2}\pi, \pi\right)$	0	-2	2	-2	0	2	0	0
π	0	$-4\sqrt{2}$	0	$-2\sqrt{2}$	0	0	0	0
$\left(\pi, \frac{3}{2}\pi\right)$	0	-2	-2	-2	0	-2	0	0
$\frac{3}{2}\pi$	$2\sqrt{2}$	$-2\sqrt{2}$	$-2\sqrt{2}$	0	0	$-2\sqrt{2}$	$2\sqrt{2}$	0
$\left(\frac{3}{2}\pi, 2\pi\right)$	2	0	0	0	2	0	2	-2
2π	2	0	0	0	4	0	0	0

in the flat space limit are easily found. For instance,

$$\lim_{k\to 0} a_{000}(\theta_H) = \begin{cases} b_{000} \\ \frac{1}{2\sqrt{2}}(b_{000} + b_{-1-1-1} + 3b_{0-1-1} + 3b_{00-1}) \\ b_{-1-1-1} \\ \frac{1}{2\sqrt{2}}(b_{-1-1-1} + b_{-2-2-2} + 3b_{-1-2-2} + 3b_{-1-1-2}) \\ b_{-2-2-2} \end{cases}$$

$$= \begin{cases} 2 & \text{for } 0 \le \theta_H < \frac{1}{2}\pi, \\ 2\sqrt{2} & \text{for } \theta_H = \frac{1}{2}\pi, \\ 0 & \text{for } \frac{1}{2}\pi < \theta_H < \frac{3}{2}\pi, \\ 2\sqrt{2} & \text{for } \theta_H = \frac{3}{2}\pi, \\ 2 & \text{for } \frac{3}{2}\pi < \theta_H \le 2\pi. \end{cases} \tag{57}$$

Some of the anomaly coefficients in the flat space limit are tabulated in Table 2.

The behavior of the anomaly coefficients for $z_L = 1.01$ depicted in Fig. 9 is understood from the limiting values tabulated in Table 2. In the RS space the anomaly coefficients $a_{n\ell m}(\theta_H)$ vary smoothly in θ_H. In the flat space limit, however, they exhibit singular behavior at $\theta_H = 0$, $\frac{1}{2}\pi$, π, and $\frac{3}{2}\pi$. This phenomenon is tightly connected with the emergence of the level crossings in the mass spectrum of the gauge and fermion fields at those points.

The contributions of the Ψ' field to anomalies are evaluated in a similar manner. The spectrum of the Ψ' field is given by Eq. (36). The mode functions $\mathbf{f}'_{Rn}(z)$ and $\mathbf{f}'_{Ln}(z)$ are obtained from $\mathbf{f}_{Rn}(z)$ and $\mathbf{f}_{Ln}(z)$ in Eqs. (49) and (50) by making a shift $\theta_H \to \theta_H + \pi$. For instance, $\mathbf{f}'_{R,2\ell}(z)$ is given by $\bar{\mathbf{f}}'^{a}_{R,2\ell}(z) = \bar{\mathbf{f}}^{b}_{R,2\ell}(z)|_{\theta_H\to\theta_H+\pi}$ for $-\pi < \theta_H < \pi$ and $\bar{\mathbf{f}}'^{b}_{R,2\ell}(z) = -\bar{\mathbf{f}}^{a}_{R,2\ell}(z)|_{\theta_H\to\theta_H+\pi}$ for $\pi < \theta_H < 2\pi$. As in the case of the anomaly coefficients $a_{nm\ell}$ coming from the Ψ field, the anomaly coefficients $a'_{nm\ell}$ coming from the Ψ' field exhibit singular behavior in the flat space limit. Some of the anomaly coefficients $a'_{nm\ell}$ in the flat space limit are tabulated in Table 3.

5. Summary and discussion

In this paper we have shown that chiral triangle anomalies flow smoothly in the scheme of $SU(2)$ GHU models in the RS space as the AB phase θ_H in the fifth dimension varies. Zero modes of $SU(2)$ doublet fermions Ψ have chiral gauge couplings at $\theta_H = 0$. Those gauge couplings change smoothly with θ_H, and they become vector-like at $\theta_H = \pi$. Although everything changes

Table 3. The anomaly coefficients $a'_{n\ell m}(\theta_H)$ due to the Ψ' field in the flat space limit. Singular behavior is observed at $\theta_H = 0$, $\frac{1}{2}\pi$, π, and $\frac{3}{2}\pi$. $a'_{n\ell m}(\theta_H)$ is related to $a_{n\ell m}(\theta_H)$ in Table 2 by $a'_{n\ell m}(\theta_H) = a_{n\ell m}(\theta_H + \pi)$ or $-a_{n\ell m}(\theta_H + \pi)$.

θ_H	a'_{000}	a'_{111}	a'_{222}	a'_{001}	a'_{011}	a'_{002}	a'_{022}	a'_{012}
0	0	$4\sqrt{2}$	0	$2\sqrt{2}$	0	0	0	0
$\left(0, \frac{1}{2}\pi\right)$	0	2	2	2	0	2	0	0
$\frac{1}{2}\pi$	$2\sqrt{2}$	$2\sqrt{2}$	$2\sqrt{2}$	0	0	$2\sqrt{2}$	$2\sqrt{2}$	0
$\left(\frac{1}{2}\pi, \pi\right)$	2	0	0	0	2	0	2	-2
π	2	0	0	0	4	0	0	0
$\left(\pi, \frac{3}{2}\pi\right)$	2	0	0	0	2	0	2	2
$\frac{3}{2}\pi$	$2\sqrt{2}$	$2\sqrt{2}$	$-2\sqrt{2}$	0	0	$-2\sqrt{2}$	$2\sqrt{2}$	0
$\left(\frac{3}{2}\pi, 2\pi\right)$	0	2	-2	2	0	-2	0	0
2π	0	$4\sqrt{2}$	0	$2\sqrt{2}$	0	0	0	0

smoothly in the RS space, the flat space limit becomes singular at $\theta_H = 0$, $\frac{1}{2}\pi$, π, and $\frac{3}{2}\pi$ where the level crossings in the mass spectrum occur in the flat $M^4 \times (S^1/Z_2)$ spacetime.

The anomaly coefficients $a^R_{n\ell m}(\theta_H)$ and $a^L_{n\ell m}(\theta_H)$ in the RS space depend on the warp factor z_L and the bulk mass parameter c of the fermion field. We have confirmed by numerical evaluation that the total anomaly coefficients $a_{n\ell m}(\theta_H) = a^R_{n\ell m}(\theta_H) + a^L_{n\ell m}(\theta_H)$ are independent of the value of c. This may have profound implications for realistic GHU models in the RS space. In the $SO(5) \times U(1) \times SU(3)$ GHU [16–18], for instance, quark–lepton multiplets are introduced such that all gauge anomalies are cancelled at $\theta_H = 0$. Each quark or lepton multiplet has its own bulk mass parameter c. In the vacuum $\theta_H \neq 0$ and the electroweak symmetry is dynamically broken. Typically, $\theta_H \sim 0.1$ and $z_L = 10^5 \sim 10^{10}$. The gauge couplings of right- and left-handed quarks or leptons change slightly at $\theta_H \neq 0$, depending on c. The universality of $a_{n\ell m}(\theta_H)$ implies that all gauge anomalies remain cancelled even at $\theta_H \neq 0$ [19,20].

Anomalies flow by an AB phase. It is known that anomalies in four dimensions are related to the global topology of the space through the index theorem [21,22]. It is challenging to understand the anomaly flow by an AB phase from the viewpoint of the index theorem [23,24]. Gauge theory in the RS space or in the flat $M^4 \times (S^1/Z_2)$ spacetime can be formulated as gauge theory on an interval ($0 \leq y \leq L$) in the fifth dimension with a special class of orbifold boundary conditions at $y = 0$ and L. In the twisted gauge in GHU the AB phase θ_H appears as a phase parameter specifying orbifold boundary conditions. Anomalies and the index theorem in orbifold gauge theory with nonvanishing θ_H have not been well understood so far. The RS space will provide a powerful tool to elucidate the anomaly flow with θ_H, as no level crossing occurs in the mass spectrum and anomalies smoothly change with θ_H, quite in contrast to the behavior in the flat space.

Acknowledgments

This work was supported in part by European Regional Development Fund-Project Engineering Applications of Microworld Physics (Grant No. CZ.02.1.01/0.0/0.0/16_ 019/0000766) (Y.O.), and by Japan Society for the Promotion of Science, Grants-in-Aid for Scientific Research, Grant No. JP19K03873 (Y.H.) and Grant No. JP18H05543 (N.Y.).

Funding

Open Access funding: SCOAP[3].

Appendix A. Basis functions

Wave functions of gauge fields and fermions are expressed in terms of the following basis functions. For gauge fields we introduce

$$\begin{aligned}
C(z;\lambda) &= \frac{\pi}{2}\lambda z z_L F_{1,0}(\lambda z, \lambda z_L),\\
S(z;\lambda) &= -\frac{\pi}{2}\lambda z F_{1,1}(\lambda z, \lambda z_L),\\
C'(z;\lambda) &= \frac{\pi}{2}\lambda^2 z z_L F_{0,0}(\lambda z, \lambda z_L),\\
S'(z;\lambda) &= -\frac{\pi}{2}\lambda^2 z F_{0,1}(\lambda z, \lambda z_L),\\
F_{\alpha,\beta}(u,v) &\equiv J_\alpha(u)Y_\beta(v) - Y_\alpha(u)J_\beta(v),
\end{aligned} \tag{A1}$$

where $J_\alpha(u)$ and $Y_\alpha(u)$ are Bessel functions of the first and second kind. They satisfy

$$\begin{aligned}
-z\frac{d}{dz}\frac{1}{z}\frac{d}{dz}\begin{pmatrix}C\\S\end{pmatrix} &= \lambda^2\begin{pmatrix}C\\S\end{pmatrix},\\
C(z_L;\lambda) = z_L, &\qquad C'(z_L;\lambda) = 0,\\
S(z_L;\lambda) = 0, &\qquad S'(z_L;\lambda) = \lambda,\\
CS' - SC' &= \lambda z.
\end{aligned} \tag{A2}$$

To express wave functions of KK modes of gauge fields, we make use of

$$\begin{aligned}
\hat{S}(z;\lambda) &= N_0(\lambda)S(z;\lambda), &\qquad \hat{C}(z;\lambda) &= N_0(\lambda)^{-1}C(z;\lambda),\\
\check{S}(z;\lambda) &= N_1(\lambda)S(z;\lambda), &\qquad \check{C}(z;\lambda) &= N_1(\lambda)^{-1}C(z;\lambda),\\
N_0(\lambda) &= \tfrac{C(1;\lambda)}{S(1;\lambda)}, &\qquad N_1(\lambda) &= \tfrac{C'(1;\lambda)}{S'(1;\lambda)}.
\end{aligned} \tag{A3}$$

For fermion fields with a bulk mass parameter c, we define

$$\begin{aligned}
\begin{pmatrix}C_L\\S_L\end{pmatrix}(z;\lambda,c) &= \pm\frac{\pi}{2}\lambda\sqrt{zz_L}F_{c+\frac{1}{2},c\mp\frac{1}{2}}(\lambda z,\lambda z_L),\\
\begin{pmatrix}C_R\\S_R\end{pmatrix}(z;\lambda,c) &= \mp\frac{\pi}{2}\lambda\sqrt{zz_L}F_{c-\frac{1}{2},c\pm\frac{1}{2}}(\lambda z,\lambda z_L).
\end{aligned} \tag{A4}$$

These functions satisfy

$$\begin{aligned}
&D_+(c)\begin{pmatrix}C_L\\S_L\end{pmatrix} = \lambda\begin{pmatrix}S_R\\C_R\end{pmatrix}, \qquad D_-(c)\begin{pmatrix}C_R\\S_R\end{pmatrix} = \lambda\begin{pmatrix}S_L\\C_L\end{pmatrix}, \qquad D_\pm(c) = \pm\frac{d}{dz} + \frac{c}{z},\\
&C_R = C_L = 1, \quad S_R = S_L = 0 \qquad \text{at } z = z_L,\\
&C_LC_R - S_LS_R = 1.
\end{aligned} \tag{A5}$$

Also, $C_L(z;\lambda,-c)=C_R(z;\lambda,c)$ and $S_L(z;\lambda,-c)=-S_R(z;\lambda,c)$ hold. To express wave functions of KK modes of fermion fields, we make use of

$$\begin{aligned}
\hat{S}_L(z;\lambda,c) &= N_L(\lambda,c)S_L(z;\lambda,c), & \hat{C}_L(z;\lambda,c) &= N_R(\lambda,c)C_L(z;\lambda,c),\\
\hat{S}_R(z;\lambda,c) &= N_R(\lambda,c)S_R(z;\lambda,c), & \hat{C}_R(z;\lambda,c) &= N_L(\lambda,c)C_R(z;\lambda,c),\\
\check{S}_L(z;\lambda,c) &= N_R(\lambda,c)^{-1}S_L(z;\lambda,c), & \check{C}_L(z;\lambda,c) &= N_L(\lambda,c)^{-1}C_L(z;\lambda,c),\\
\check{S}_R(z;\lambda,c) &= N_L(\lambda,c)^{-1}S_R(z;\lambda,c), & \check{C}_R(z;\lambda,c) &= N_R(\lambda,c)^{-1}C_R(z;\lambda,c),\\
N_L(\lambda,c) &= \tfrac{C_L(1;\lambda,c)}{S_L(1;\lambda,c)}, & N_R(\lambda,c) &= \tfrac{C_R(1;\lambda,c)}{S_R(1;\lambda,c)}.
\end{aligned} \tag{A6}$$

Appendix B. Mode functions of fermion fields with $c < 0$

When the bulk mass parameter c of a fermion field $\Psi(x,z)$ is negative, the roles of right-handed and left-handed components are interchanged compared with those of a field with positive c. In the KK expansions in Eq. (48) the mode functions $\mathbf{f}_{Rn}(z)$ and $\mathbf{f}_{Ln}(z)$ are given, for $c<0$, by

$$\mathbf{f}_{R0}(z)=\bar{\mathbf{f}}^a_{R0}(z);$$

$$\mathbf{f}_{R,2\ell-1}(z)=\begin{cases}
\bar{\mathbf{f}}^a_{R,2\ell-1}(z) & \text{for } -\pi<\theta_H<\pi,\\
\bar{\mathbf{f}}^b_{R,2\ell-1}(z) & \text{for } 0<\theta_H<2\pi,\\
-\bar{\mathbf{f}}^a_{R,2\ell-1}(z) & \text{for } \pi<\theta_H<3\pi,\\
-\bar{\mathbf{f}}^b_{R,2\ell-1}(z) & \text{for } 2\pi<\theta_H<4\pi,\\
\bar{\mathbf{f}}^a_{R,2\ell-1}(z) & \text{for } 3\pi<\theta_H<5\pi
\end{cases} \qquad (\ell=1,2,3,\ldots);$$

$$\mathbf{f}_{R,2\ell}(z)=\begin{cases}
\bar{\mathbf{f}}^c_{R,2\ell}(z) & \text{for } -\pi<\theta_H<\pi,\\
\bar{\mathbf{f}}^d_{R,2\ell}(z) & \text{for } 0<\theta_H<2\pi,\\
-\bar{\mathbf{f}}^c_{R,2\ell}(z) & \text{for } \pi<\theta_H<3\pi,\\
-\bar{\mathbf{f}}^d_{R,2\ell}(z) & \text{for } 2\pi<\theta_H<4\pi,\\
\bar{\mathbf{f}}^c_{R,2\ell}(z) & \text{for } 3\pi<\theta_H<5\pi
\end{cases} \qquad (\ell=1,2,3,\ldots) \tag{B1}$$

and

$$\mathbf{f}_{L,2\ell}(z)=\begin{cases}
\bar{\mathbf{f}}^a_{L,2\ell}(z) & \text{for } -\pi<\theta_H<\pi,\\
\bar{\mathbf{f}}^b_{L,2\ell}(z) & \text{for } 0<\theta_H<2\pi,\\
-\bar{\mathbf{f}}^a_{L,2\ell}(z) & \text{for } \pi<\theta_H<3\pi,\\
-\bar{\mathbf{f}}^b_{L,2\ell}(z) & \text{for } 2\pi<\theta_H<4\pi,\\
\bar{\mathbf{f}}^a_{L,2\ell}(z) & \text{for } 3\pi<\theta_H<5\pi
\end{cases} \qquad (\ell=0,1,2,\ldots);$$

$$\mathbf{f}_{L,2\ell-1}(z)=\begin{cases}
\bar{\mathbf{f}}^c_{L,2\ell-1}(z) & \text{for } -\pi<\theta_H<\pi,\\
\bar{\mathbf{f}}^d_{L,2\ell-1}(z) & \text{for } 0<\theta_H<2\pi,\\
-\bar{\mathbf{f}}^c_{L,2\ell-1}(z) & \text{for } \pi<\theta_H<3\pi,\\
-\bar{\mathbf{f}}^d_{L,2\ell-1}(z) & \text{for } 2\pi<\theta_H<4\pi,\\
\bar{\mathbf{f}}^c_{L,2\ell-1}(z) & \text{for } 3\pi<\theta_H<5\pi
\end{cases} \qquad (\ell=1,2,3,\ldots). \tag{B2}$$

Here, $\bar{\mathbf{f}}^a_{Rn}(z)$, $\bar{\mathbf{f}}^b_{Rn}(z)$, etc. are given in Eq. (52).

References

[1] Y. Hosotani, Phys. Lett. B **126**, 309 (1983).
[2] A. T. Davies and A. McLachlan, Phys. Lett. B **200**, 305 (1988).
[3] Y. Hosotani, Ann. Phys. (N.Y.) **190**, 233 (1989).
[4] A. T. Davies and A. McLachlan, Nucl. Phys. B **317**, 237 (1989).
[5] H. Hatanaka, T. Inami, and C. S. Lim, Mod. Phys. Lett. A **13**, 2601 (1998).
[6] H. Hatanaka, Prog. Theor. Phys. **102**, 407 (1999).
[7] M. Kubo, C. S. Lim, and H. Yamashita, Mod. Phys. Lett. A **17**, 2249 (2002).

[8] S. Funatsu, H. Hatanaka, Y. Hosotani, Y. Orikasa, and N. Yamatsu, Phys. Rev. D **104**, 115018 (2021).
[9] S. L. Adler, Phys. Rev. **177**, 2426 (1969).
[10] J. S. Bell and R. Jackiw, Nuovo Cim. A **60**, 47 (1969).
[11] K. Fujikawa, Phys. Rev. Lett. **42**, 1195 (1979).
[12] K. Fujikawa, Phys. Rev. D **21**, 2848 (1980).
[13] A. Falkowski, Phys. Rev. D **75**, 025017 (2007).
[14] Y. Hosotani and Y. Sakamura, Prog. Theor. Phys. **118**, 935 (2007).
[15] L. Randall and R. Sundrum, Phys. Rev. Lett. **83**, 3370 (1999).
[16] Y. Hosotani, S. Noda, and N. Uekusa, Prog. Theor. Phys. **123**, 757 (2010).
[17] S. Funatsu, H. Hatanaka, Y. Hosotani, Y. Orikasa, and T. Shimotani, Phys. Lett. B **722**, 94 (2013).
[18] S. Funatsu, H. Hatanaka, Y. Hosotani, Y. Orikasa, and N. Yamatsu, Phys. Rev. D **99**, 095010 (2019).
[19] C. Bouchiat, J. Iliopoulos, and Ph. Meyer, Phys. Lett. B **38**, 519 (1972).
[20] D. J. Gross and R. Jackiw, Phys. Rev. D **6**, 477 (1972).
[21] M. F. Atiyah and I. M. Singer, Ann. Math. **87**, 484 (1968).
[22] M. F. Atiyah, V. K. Patodi, and I. M. Singer, Math. Proc. Camb. Phil. Soc. **77**, 43 (1975).
[23] H. Fukaya, T. Onogi, and S. Yamaguchi, Phys. Rev. D **96**, 125004 (2017).
[24] E. Witten and K. Yonekura, arXiv:1909.08775 [hep-th] [Search inSPIRE].